CHAPTER IV

A PHYSICOCHEMICAL CHARACTERISATION

4.1. The stoichiometric problem

The functional stoichiometries and subunit arrangements issues of the 5-HT_3 receptors are still unresolved subjects. The 5-HT_3 receptors stoichiometry is a complicated matter because of the presence of five subunits (A-E), not to mention all the existing subunit sequence isoforms and splice variants [Yaakob *et al*., 2011]. The many possible different compositions and stoichiometries, and subsequently, the many possible interfaces could provide non equivalent ligand binding sites both for agonists and antagonists, thus largely affecting the pharmacological modulation of this receptor.

Given the physiological and therapeutic significance of the 5-HT_3 receptor, studies on receptor stoichiometry may therefore help the research in developing more selective and highly successful antagonists.

Among the five different 5-HT_3R subunits, subunits A and B have been largely studied and characterised, while subunits C, D, and E have been sequenced but not yet fully characterised [Barnes *et al*., 2009; Niesler *et al*., 2003]. As mentioned in the introduction of this thesis, the 5-HT_3A subunit is capable of forming functional homopentameric receptors; on the contrary, 5-HT_3B is unable to express as a homopentamer. However, if co-expressed with subunit A it was found to build functional B/A heteropentamers. The subunit stoichiometry in the heteropentameric receptor is debated: AFM studies have demonstrated that the heteropentamer has a 2A:3B stoichiometry with a BBABA arrangement [Barrera *et al*., 2005], where no AA interface is present; while experimental site directed mutagenesis studies support the requirements of at least one AA interface for any 5-HT_3R to be functional [Lochner & Lummis, 2010; Thompson *et al.*, 2011]. Therefore, it was suggested that the 5-HT_3B subunit does not contribute to the binding site and 5-HT_3AB receptors presumably contain at least one AA interface.

Thus, the composition of the receptors, by considering different stoichiometries of subunits A and B only, may vary largely, with the possible permutations being: AAAAA, BAAAA, BBAAA, BABAA, BBBAA, BABBA, BBBBA (BBBBB is not considered since it is known not to be functional) [Yaakob *et al*., 2011].

Although little is known about the functional features of the remaining subunits C, D, and E, they are apparently able to form functional heteropentameric receptors if co-expressed with subunit A, as it is also the case of the B subunit [Niesler *et al*., 2007; Holbrook *et al*., 2009], complicating further on the stoichiometry.

In addition to the experimental studies [Barrera *et al*., 2005; Lochner & Lummis, 2010; Thompson *et al*., 2011], further several computational studies took into question the problem of the stoichiometry by means of either the analysis of the subunits assembling or the study of protein-protein interactions. This study were performed both indirectly on the nAChR, the prototypical Cys-loop receptor, and directly on the 5-HT_3R. In particular, Ortells and Barrantes [2008] have tackled the problem of the assembly mechanism of the LGICs by analysing the complementarity in shape and physicochemical properties of the various subunit interfaces. Although they briefly take into account 5-HT_3R A and B subunits, their work is mainly focussed on the detailed analysis of various nAChR subunits in the attempt to predict whether the β1δα1γα1 receptor assembles following the so-called "heterodimer model" (which proposes that two dimers (δα1 and γα1) are formed independently and then associate with each other and with the remaining β1 subunit) or the alternative "sequential model" (which hypothesises that first heterodimers of different compositions are assembled to rapidly form the α1β1γ trimer and subsequently add the δ and the second α1 subunit).

Moreover, the 5-HT_3R AA interface has been recently analysed in our laboratory and characterised using a Computer Aalanine Scanning Mutagenesis (CASM) protocol flanked by MD simulations [De Rienzo *et al*., 2012]. The combined MD-CASM protocol proved to be useful to point out the structurally and energetically critical points on the receptor interface, whose perturbation by ligands might promote or impair the channel activation or the protein functionality. In particular, the presence of an aromatic cluster, which is formed by residues **W178** (hot spot in the *principal* subunit), and **Y83** (hot spot in the *complementary* subunit), **Y68**, **W85** and **Y148** (warm spot in the *complementary* subunit) and is located in the middle of the binding interface (Figure 38). This is the "hot centre" of the protein-protein interaction and is probably involved in the correct assembling of the

extracellular part of the receptor. In addition, analysis of the coupling of agonist/antagonist binding to channel activation/inactivation suggested that two of these hot-centre residues, i.e. **W178** and **Y148**, are key points of the binding/activation mechanism.

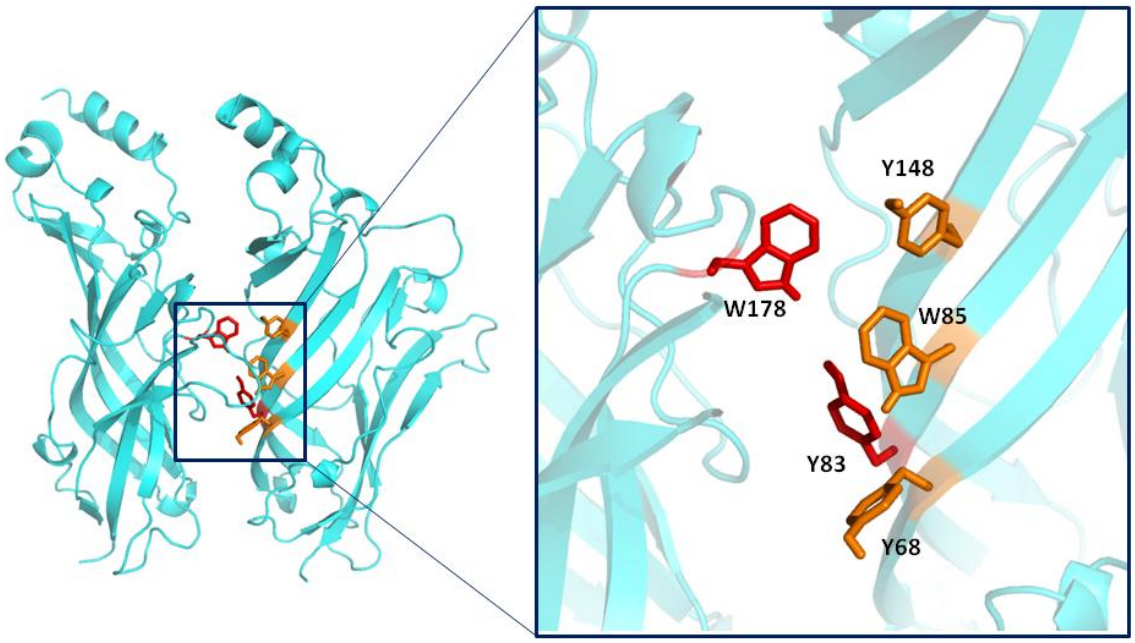

Figure 38- The 5-HT_3R AA dimer with its "hot centre" of the protein-protein interaction focussed on in the blue square. Interface residues are highlighted in stick: hot spot are in red; warm spot in orange.

Experimental and computational studies are performed mainly on the 5-HT_3R extracellular domain, whereas the TM and the IC receptor domains are far less characterised. A deeper knowledge of these latter portions could provide useful hints for the complete characterisation of the receptor.

4.2 Aim of work

The aim of this work is to get new insights into the possible stoichiometric composition of the 5-HT_3 functional receptors. The many different possible interfaces that can form the

5-HT_3Rs are studied from a physicochemical point of view (in particular, the hydrophobic and electrostatic properties) in order to predict the role played by the extracellular moieties of the A and B subunits in the formation of functional or non functional receptors. The conclusions and hypotheses advanced are further extended to the additional C, D, and E subunits.

Moreover, the 3D homology models of the TM and IC regions for the human subunits 5-HT_3A to 5-HT_3E are built and assembled into homopentameric (5-HT_3A, 5-HT_3B, 5-HT_3C, 5-HT_3D and 5-HT_3E) and heteropentameric (5-HT_3AB, 5-HT_3AC, 5-HT_3AD and 5-HT_3AE) receptors. A detailed comparison of the receptor subunit sequences and structures is carried out and, successively, the molecular electrostatic potential and the energetic profile of a cation along the pore channel of the homopentameric and heteropentameric receptors are computed and analysed.

As a whole, the analysis of the physicochemical properties of the 5-HT_3Rs will help us to interpret experimental data, to suggest possible explanations about the different behaviour shown by different receptors within the 5-HT_3 receptor family, and to make hypotheses about the correlations of the receptor stoichiometry and functionality.

To our knowledge, no 3D structural model of the 5-HT_3 B, C, D and E subunit TM and IC domains has been built and reported in the literature, so far.

4.3 Methods and Materials

4.3.1 The EC domain interfaces

The 5-HT_{3A}R (homomeric) and 5-HT_{3AB}R (heteromeric) structures built and minimised as described by Moura Barbosa *et al*. [2010] were used to extract the following subunit interfaces: AA (from the homopentamer), AB, BA and BB (from the heteropentamer).

The sequences for the EC domains of the 5-HT_3R subunit C, D, and E were extracted from the UniProt/SwissProt databank with UniProtKB accession codes: Q8WXA8 (subunit C),

Q70Z44 (subunit D), and A5X5Y0 (subunit E). The multiple alignment of the five 5-HT_3R subunits was obtained with ClustalW [Thompson *et al.*, 1994] using BLOSUM matrix, a gap pen penalty of 10, a gap extension penalty of 0.20, and a gap distances penalty of 5. This alignment is shown in Figure 39 together with sequence similarity percentages.

Sequence similarity percentage

	A	B	C	D	E
A	100				
B	48	100			
C	35	30	100		
D	21	15	42	100	
E	35	32	74	39	100

Figure 39- ClustalW multiple sequence alignment of the EC domains of the five 5-HT_3R subunits A, B, C, D and E. The prediction of the secondary structure is reported for all the five sequences: *C* = random structure; *H* = α-helix; *E* = β-strand. The sequence similarities are also reported. Gray underlined bold characters indicate the residues forming the "hot-core" of the protein interface. Code: * = conserved residue in all sequences; : = different but highly conserved (very similar) residues; . = different residues that are somewhat similar.

4.3.3 TM and IC domain models building and refinements

The amino acid sequences of the TM and IC domains of the human 5-HT_3 receptor subunit A (UniProtKB entry: P46098), subunit B (UniProtKB entry: O95264), subunit C (UniProtKB entry: Q8WXA8), subunit D (UniProtKB entry: Q70Z44) and subunit E (UniProtKB entry: A5X5Y0) were extracted from the UniProtKB/Swiss-Prot (The UniProt Consortium, 2008) protein sequence database. These sequences were used to build structural homology models of the TM and IC portions of the human homomeric and heteromeric 5-HT_3 receptors. The available structures of the nAChR from *Torpedo Marmorata* (PDB entry: 2BG9) [Unwin, 2005] and the ELIC (PDB entry: 2VL0) [Hilf & Dutzler, 2008] were used as templates.

The sequence identity between ELIC and the 5-HT_3A subunit is lower (16%) than that between nAChR and the 5-HT_3A subunit (i.e. 27% and 22% for nAChR subunit β and ε, respectively), however both the structures were used because of the higher ELIC resolution with respect to that of nAChR (3.3 vs 4.0 Å). The GLIC and GluCl structures, which have a sequence identity (to 5-HT_3A) similar to that of ELIC (16-18%) but higher resolutions (2.90 Å and 3.26 Å), have not been taken into account because, in contrast to the other two structures, they show an open-pore folding [Bocquet *et al.*, 2009; Hibbs & Gouaux, 2011; Zhu & Hummer, 2012].

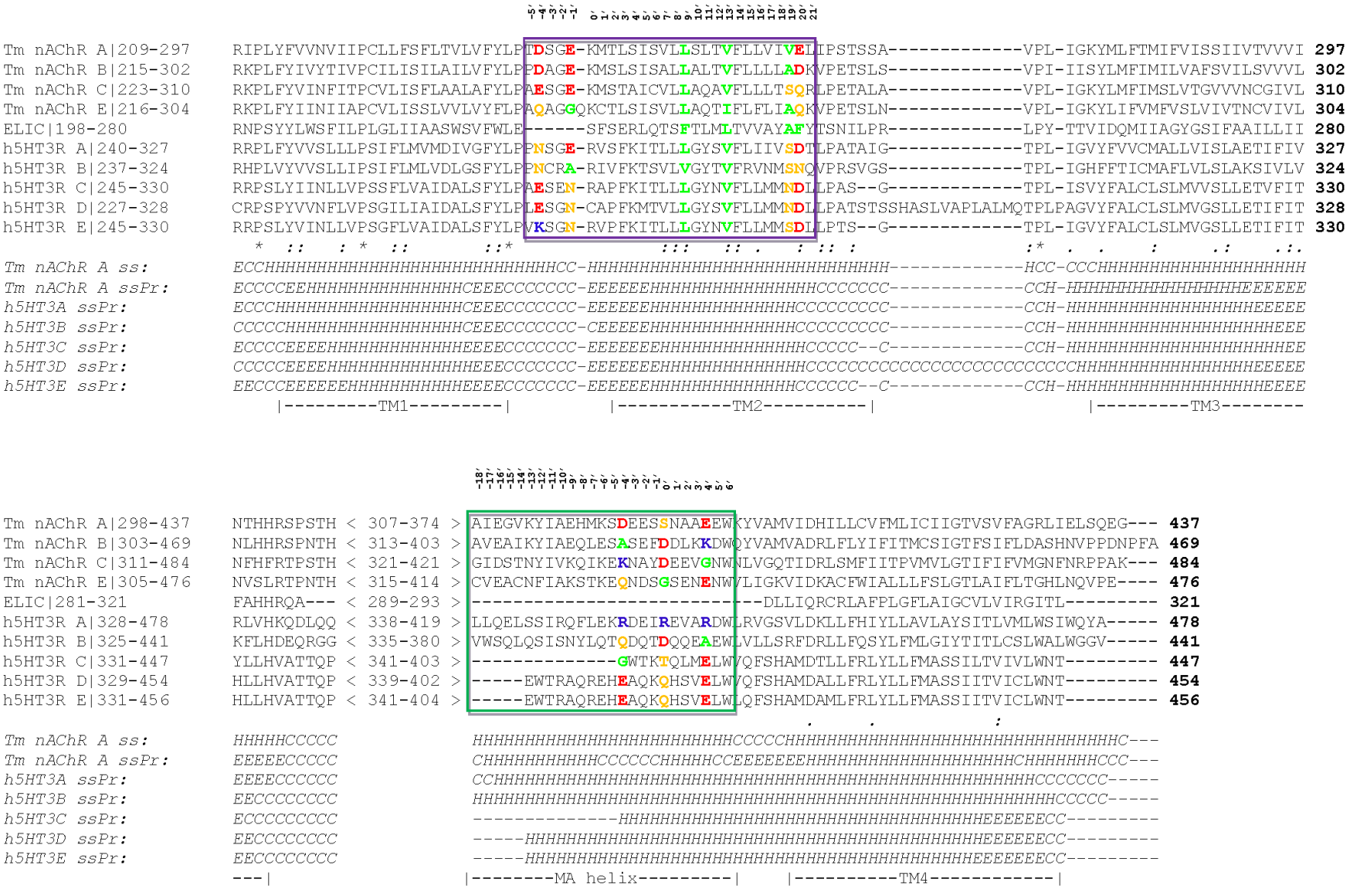
Tm nAChR A|209-297 RIPLYFVVNVIIPCLLFSFLTVLVFYLPTDSGE-KMTLSISVLLSLTVFLLVIVELIPSTSSA----------VPL-IGKYMLFTMIFVISSIIVTVVVI 297
Tm nAChR B|215-302 RKPLFYIVYTIVPCILISILAILVFYLPPDAGE-KMSLSISALLALTVFLLLLADKVPETSLS----------VPI-IISYLMFIMILVAFSVILSVVVL 302
Tm nAChR C|223-310 RKPLFYVINFITPCVLISFLAALAFYLPAESGE-KMSTAICVLLAQAVFLLLTSQRLPETALA----------VPL-IGKYLMFIMSLVTGVVVNCGIVL 310
Tm nAChR E|216-304 RKPLFYIINIIAPCVLISSLVVLVYFLPAQAGGQKCTLSISVLLAQTIFLFLIAQKVPETSLN----------VPL-IGKYLIFVMFVSLVIVTNCVIVL 304
ELIC|198-280 RNPSYYLWSFILPLGLIIAASWSVFWLE------SFSERLQTSFTLMLTVVAYAFYTSNILPR----------LPY-TTVIDQMIIAGYGSIFAAILLII 280
h5HT3R A|240-327 RRPLFYVVSLLLPSIFLMVMDIVGFYLPPNSGE-RVSFKITLLLGYSVFLIIVSDTLPATAIG----------TPL-IGVYFVVCMALLVISLAETIFIV 327
h5HT3R B|237-324 RHPLVYVVSLLIPSIFLMLVDLGSFYLPPNCRA-RIVFKTSVLVGYTVFRVNMSNQVPRSVGS----------TPL-IGHFFTICMAFLVLSLAKSIVLV 324
h5HT3R C|245-330 RRPSLYIINLLVPSSFLVAIDALSFYLPAESEN-RAPFKITLLLGYNVFLLMMNDLLPAS--G----------TPL-ISVYFALCLSLMVVSLLETVFIT 330
h5HT3R D|227-328 CRPSPYVVNFLVPSGILIAIDALSFYLPLESGN-CAPFKMTVLLGYSVFLLMMNDLLPATSTSSHASLVAPLALMQTPLPAGVYFALCLSLMVGSLLETIFIT 328
h5HT3R E|245-330 RRPSLYVINLLVPSGFLVAIDALSFYLPVKSGN-RVPFKITLLLGYNVFLLMMSDLLPTS--G----------TPL-IGVYFALCLSLMVGSLLETIFIT 330
Tm nAChR A ss: ECCHHHHHHHHHHHHHHHHHHHHHHHHHHHCC-HHHHHHHHHHHHHHHHHHHHHHHHHHH----------HCC-CCCHHHHHHHHHHHHHHHHH
Tm nAChR A ssPr: ECCCCEEHHHHHHHHHHHHHHHCEEECCCCCCC-EEEEEEHHHHHHHHHHHHHHHHCCCCCCC----------CCH-HHHHHHHHHHHHHHHHEEEEEE
h5HT3A ssPr: ECCCHHHHHHHHHHHHHHHHHCEEECCCCCCC-EEEEEEHHHHHHHHHHHHHHHCCCCCCCCC----------CCH-HHHHHHHHHHHHHHHHHHEEEEE
h5HT3B ssPr: CCCCCHHHHHHHHHHHHHHHHCEEECCCCCCC-CEEEEEHHHHHHHHHHHHHHHCCCCCCCCC----------CCH-HHHHHHHHHHHHHHHHHHHEEE
h5HT3C ssPr: ECCCCEEEEHHHHHHHHHHHHEEEECCCCCCC-EEEEEEEHHHHHHHHHHHHHHCCCCC--C----------CCH-HHHHHHHHHHHHHHHHHHHHEE
h5HT3D ssPr: CCCCCEEEEHHHHHHHHHHHHHEEECCCCCCC-EEEEEEEHHHHHHHHHHHHHHCCCCCCCCCCCCCCCCCCCCCCCCCCHHHHHHHHHHHHHHHHEEEEE
h5HT3E ssPr: EECCCEEEEEEHHHHHHHHHHHEEEECCCCCCC-EEEEEEHHHHHHHHHHHHHHCCCCCC--C----------CCH-HHHHHHHHHHHHHHHHHHHEEEE
|---------TM1---------| |-----------TM2----------| |---------TM3---------
Tm nAChR A|298-437 NTHHRSPSTH < 307-374 > AIEGVKYIAEHMKSDEESSNAAEEWKYVAMVIDHILLCVFMLICIIGTVSVFAGRLIELSQEG--- 437
Tm nAChR B|303-469 NLHHRSPNTH < 313-403 > AVEAIKYIAEQLESASEFDDLKKDWQYVAMVADRLFLYIFITMCSIGTFSIFLDASHNVPPDNPFA 469
Tm nAChR C|311-484 NFHFRTPSTH < 321-421 > GIDSTNYIVKQIKEKNAYDEEVGNWNLVGQTIDRLSMFIITPVMVLGTIFIFVMGNFNRPPAK--- 484
Tm nAChR E|305-476 NVSLRTPNTH < 315-414 > CVEACNFIAKSTKEQNDSGSENENWVLIGKVIDKACFWIALLLFSLGTLAIFLTGHLNQVPE---- 476
ELIC|281-321 FAHHRQA--- < 289-293 > ----------DLLIQRCRLAFPLGFLAIGCVLVIRGITL--------- 321
h5HT3R A|328-478 RLVHKQDLQQ < 338-419 > LLQELSSIRQFLEKRDEIREVARDWLRVGSVLDKLLFHIYLLAVLAYSITLVMLWSIWQYA----- 478
h5HT3R B|325-441 KFLHDEQRGG < 335-380 > VWSQLQSISNYLQTQDQTDQQEAEWLVLLSRFDRLLFQSYLFMLGIYTITLCSLWALWGGV----- 441
h5HT3R C|331-447 YLLHVATTQP < 341-403 > ----------GWTKTQLMELWVQFSHAMDTLLFRLYLLFMASSILTVIVLWNT--------- 447
h5HT3R D|329-454 HLLHVATTQP < 339-402 > -----EWTRAQREHEAQKQHSVELWVQFSHAMDALLFRLYLLFMASSIITVICLWNT--------- 454
h5HT3R E|331-456 HLLHVATTQP < 341-404 > -----EWTRAQREHEAQKQHSVELWLQFSHAMDAMLFRLYLLFMASSIITVICLWNT--------- 456
Tm nAChR A ss: HHHHHCCCCC HHHHHHHHHHHHHHHHHHHHHHHHHCCCCCHHHHHHHHHHHHHHHHHHHHHHHHHHHHHC---
Tm nAChR A ssPr: EEEEECCCCC CHHHHHHHHHHCCCCCCHHHHCCEEEEEEEHHHHHHHHHHHHHHHHHHHHCHHHHHHCCC---
h5HT3A ssPr: EEEECCCCCC CCHHHHHHHHHHHHHHHHHHHHHHHHHHHHHHHHHHHHHHHHHHHHHHHHHHCCCCCCC-----
h5HT3B ssPr: EECCCCCCCC HHHHHHHHHHHHHHHHHHHHHHHHHHHHHHHHHHHHHHHHHHHHHHHHHHHHHHHCCCCC-----
h5HT3C ssPr: ECCCCCCCCC ----------HHHHHHHHHHHHHHHHHHHHHHHHHHHHHHHHHHHEEEEEECC---------
h5HT3D ssPr: EECCCCCCCC -----HHHHHHHHHHHHHHHHHHHHHHHHHHHHHHHHHHHHHHHHHHHEEEEEECC---------
h5HT3E ssPr: EECCCCCCCC -----HHHHHHHHHHHHHHHHHHHHHHHHHHHHHHHHHHHHHHHHHHHEEEEEECC---------
---| |--------MA helix---------| |----------TM4----------|

Figure 40- Multiple sequence alignment between the structures of the four different subunits (A, B, C, E) of the nicotinic acetylcholine receptor from *Torpedo marmorata* (Tm nAChR; PDB code: 2BG9), the structure of a subunit of the pentameric ligand-gated ion channel from *Erwinia chrysanthemi* (ELIC; PDB code: 2VL0) and the amino acid sequences of the five 5-HT_3R subunits A, B, C, D and E, manually adjusted on the basis of the ClustalW and structural alignments, and the prediction of the secondary structure. The prediction of the secondary structure (*ssPr*) is reported for the Tm nAChR A and for all the five human 5-HT_3 sequences: *C* = random structure; *H* = α-helix; *E* = β-strand. Moreover the secondary structure of the PDB structure of TM nAChR A is reported (*Tm nAChR A ss*). Transmembrane and intracellular regions are underlined (TM1, TM2, TM3, TM4, MA helix). The violet square contains the approximate TM1-TM2 linker and the TM2 region: within the alignment, the important residues for ion selectivity and gating [Kienker *et al*., 1994; Gunthorpe & Lummis, 2001; Thompson & Lummis, 2003; Yakel *et al*., 1993; Paniker *et al*., 2002; Dang *et al*., 2000; Livesey *et al.*, 2008] are highlighted with different colours: basic amino acids are blue, acidic are red, polar are orange and non-polar are green. The prime numbering scheme for TM2 residues was described previously [Miller, 1989]. The green square contains the MA-helix region in the IC domain: within the alignment, the important residues for ion conductivity [Livesey *et al*., 2008; Kelley *et al*., 2003; Hales *et al*., 2006; Peters *et al*., 2010] are highlighted with different colours: basic amino acids are blue, acidic are red, polar are orange and non-polar are green. The prime numbering scheme for MA-helix residues was described previously (Hales *et al.*, 2006). Code: * = conserved residue in all sequences; : = different but highly conserved (very similar) residues; . = different residues that are somewhat similar.

A multiple alignment of these sequences, together with the sequences of the five chains of the nAChR structure and the ELIC subunit, was generated with ClustalW [Thompson *et al.*, 1994], using default parameters. A structure-based alignment was also performed using the software MODELLER v. 9.10 [Sali & Blundell, 1993]. Putative helices were predicted by means TMHMM2 [Krogh *et al*., 2001] and PSIPRED [Buchan *et al*., 2012; Jones, 1999]. Manual adjustments were necessary in the structural alignment to obtain a good agreement between the four transmembrane α-helices (TM1, TM2, TM3 and TM4) and the intracellular α-helix (MA-helix) of nAChR, ELIC and the secondary structure prediction for 5-HT_3R (see Figure 40). The major shifts were done in the final part of the sequences, in particular to align the MA-helix.

In the nAChR structure, the region between TM3 and TM4 is only partially solved at the electron microscopy: in fact, with the exception of the MA-helix, the atomic coordinates of most of this region are not available [Unwin, 2005]. In the 5-HT_3R sequences there is a

long insertion corresponding to that region, which has been deleted from the sequence-structure alignment, so the residues included for each subunit are the following: A from 240 to 337 and from 418 to 478; B from 237 to 334 and from 381 to 441; C from 245 to 340 and from 405 to 447; D from 227 to 338 and from 403 to 454; E from 245 to 340 and from 405 to 456 (Figure 40).

Modelling of the 5-HT_3A subunit was performed with the software MODELLER v 9.10 [Sali & Blundell, 1993] using all the five chains of the nAChR structure and one chain of the ELIC structure (the five ELIC subunit are all identical) as templates. Twenty 3D models were generated for the 5-HT_3A subunit and checked against the available structural experimental information, such as the location of a few residues known to be involved in important functional roles by mutagenesis experiments. The positions of these key residues were checked for all the modelled 5-HT_3A subunit structures in order to reject those structures which did not agree with the experimental information.

Subsequently, the 3D structures selected were also evaluated with the global G-factors and the Ramachandran plot residue distribution from the software PROCHECK [Laskowski *et al.*, 1993], the objective function from MODELLER [Sali & Blundell, 1993], the error values from ERRAT [Colovos & Yates, 1993], and the global quality indicators from WHAT_CHECK [Hooft *et al*., 1996; Vriend, 1990].

The 3D structures with the best agreement with experimental data [Barnes *et al.*, 2009 and references therein] and the best technical evaluation score were selected and used for further analyses.

The 5-HT_3A model selected was used as template for modelling the human 5-HT_3B, 5-HT_3C, 5-HT_3D and 5-HT_3E TM and IC domains. Ten model structures were generated for each of these subunits, whose quality was assessed with the same technical checks used to select the 5-HT_3A model. In addition, since nearly no experimental info is available for these subunit structures, the structural checks were performed taking into account the residues corresponding (in the multiple sequence alignment) to the 5-HT_3A residues known to be relevant for function and/or structure.

Once selected the best 3D model structure for each subunit, the homopentamer receptors 5-HT_3A, 5-HT_3B, 5-HT_3C, 5-HT_3D and 5-HT_3E and the heteropentamer receptor 5-HT_3AB, 5-HT_3AC, 5-HT_3AD and 5-HT_3AE were built using the known pentameric structural constraints of the nAChR (PDB: 2BG9). The arrangement of the heteromeric receptors follows the AFM study carried out by Barrera and co-workers [Barrera et al., 2005] in which they demonstrated that the 5-HT_3AB heteropentamer has a 2A:3B stoichiometry with a BBABA arrangement. Consequently, the stoichiometry used for the other heteropentamers was the same: CCACA, DDADA, EEEAEA. Nevertheless, recent works [Lochner & Lummis, 2010; Thompson et al. 2011] based both on modelling and experimental site-directed mutagenesis studies on the 5-HT_3R, demonstrated the requirements of at least one AA interface for any 5-HT_3R to be functional. To test this hypothesis, the 5-HT_3AB receptor, which is the most studied among the different heteropentamers, was also built considering all the other possible stoichiometries (ABBBB, AABBB, AAABB, AAAAB, ABABA). Briefly, the modelled structure of every subunit was superimposed to each of the five subunits of the TM and IC domains of the nAChR structure, to obtain a pentamer made of five identical subunits A or B or C or D or E. The heteromeric structures were built with the same procedure, superimposing either the modelled subunit A or one of the modelled subunits B, C, D, and E, onto each nAChR subunit in order to reproduce the desired arrangement.

4.3.4 Calculation of physicochemical parameters relevant for protein-protein interaction in the EC domains

The physicochemical study of the dimer interface surfaces was performed using the MolSurfer package [Gabdoulline *et al.*, 1999, 2003], which includes the analysis of the electrostatic, hydrophobic and shape complementarity.

Using as input the individual structure of each monomer in the dimer, the MolSurfer package generates 3D surface-surface interface maps which are then projected on a 2D space. The interface between the two macromolecules (protein/protein) is mapped by

Adsi [Gabdoulline *et al*., 1999, 2003], and the molecular properties of each protein are projected onto every point of the interface (these are the properties assigned to the closest atom to the point). The interface between the macromolecules is considered a contact surface if the surface-to-surface distance is less than 5 Å (considering van der Waals surfaces of the two subunits). The values of the surface-to-surface distances, hydrophobicities and electrostatic potentials are displayed at each point of the interface surface. Surface to surface distance is an indicator of the interface shape complementarity.

The molecular electrostatic potential (MEP) of each isolated protein was computed with the UHBD [Madura *et al.*, 1995] program by solving the finite difference linearised Poisson-Boltzmann equation and the potential values were interpolated at each interface point. The parameters used are: the Amber force field to describe atomic radii and charges [Dolinsky *et al*., 2004, 2007], a grid dimension of 99x99x99 $Å^3$ with 1 Å grid spacing, an ionic strength of 150 mM, a protein dielectric constant of 5 and a solvent dielectric constant of 80, an ion radius of 1.5 Å and Van der Waals surface to separate the protein and the solvent. Residue hydrophobicities were assigned according to the residue name and the parameters in Eisenberg *et al*. [1982].

Besides the hydrophobicities and the electrostatic potentials, also their similarity indices, namely HSI (Hydrophobicity Similarity Index) and EPSI (Electrostatic Potential Similarity Index), are computed by MolSurfer and mapped onto the 2D projection of the dimer interface [Gabdoulline *et al*., 1999, 2003].

Electrostatic complementarity at the 5-HT_3R dimer interfaces is quantified by negative values (EPSI between 0 and -1; red areas) of the electrostatic potentials similarity index: the more negative is the EPSI, the higher is the surface electrostatic potential (EP) complementarity. In fact, a negative EPSI indicates that the residues on the two interacting protein surfaces are characterised by opposite charged areas, i.e. there are positive residues on one surface and negative residues on the other surface. A positive value of EPSI (blue areas on the 2D EPSI map) indicates instead that the residues on the two surfaces are similarly charged (which means no electrostatic complementarity). On

the contrary, the hydrophobic complementarity at the dimer interface is higher when the HSI assumes positive values (blue areas on the 2D map): this in fact means that the hydrophobic properties of the two interacting protein surfaces are similar, which is a determinant requirement for hydrophobic complementarity. Negative values (corresponding to red areas on the 2D maps) instead indicate that the two surfaces have different hydrophobic properties (no hydrophobic complementary).

4.3.5 Electrostatic potentials of the TM-IC domains

The electrostatic potential of each pentamer was computed using the APBS software [Baker *et al*., 2011] through solution of the linear Poisson-Boltzmann (PB) equation, a continuum model for describing electrostatic interactions between molecular solutes in a salty and aqueous media. The PyMOL Molecular Graphics System, Version 1.2r3pre [DeLano, 2008] was used as graphic interface for APBS (APBS Tools2.1) [Lerner & Carlson, 2006] and for the visualization of the resulting electrostatic potentials. The parameters used are: a grid of 137x136x163 $Å^3$ with 161x161x193 grid points, Single Debye-Hückel sphere as boundary conditions, an ionic concentration of 0.150 M, a protein dielectric constant of 2 and a solvent dielectric constant of 78, a solvent radius of 1.4 Å and a system temperature of 310 K. Radii and charges were assigned using the web service PDB2PQR [Dolinsky *et al*., 2004, 2007], choosing the PARSE force field, optimised for implicit solvent calculations, before APBS calculations. The ±1 kT/e electrostatic potential surfaces of each pentamer were plotted on the solvent-accessible surface.

4.3.6 Energy profile calculations at the TM-IC domains level

Electrostatics calculations based on the Poisson-Boltzmann (PB) equation provide an approximate evaluation of the energy profile of an ion passing through a channel [Kaihsu *et al.*, 2008].

PB calculations were performed using the software package APBS [Backer *et al*., 2001], to estimate the electrostatic contribution to the energy barrier for a calcium ion placed at successive points along the pore axis. The analysis of the pore were performed by means of the HOLE program [Smart *et al*., 1996] to obtain both the pore radius profile and the sample points along the pore axis to be probed by the Ca^{2+} ion. The web service PDB2PQR [Dolinsky *et al*., 2004, 2007] was used to assign radii and charges for all of the atoms, as previously described.

More precisely, the analysis of the pore performed by HOLE furnishes the coordinates of the pore axis: the pore axis lies parallel to the z-axis with coordinates (63 Å, 63 Å, z), where z ranges between 50 Å and 110 Å. To have a detailed-enough description of the pore, the sample points where to place the Ca^{2+} ion were chosen to be 2 Å apart along the pore-axis, i.e. the sampled points were: P1 (63, 63, 50), P2 (63, 63, 52), P3 (63, 63, 54)…. P31 (63, 63, 110). A cation with charge +2 and radius 1.86 Å, equivalent to the Born radius of calcium [Rashin & Hoing, 1985], was successively placed at each sample point. A single-point energy evaluation was performed and repeated for every of these sample positions, as described by Beckstein and co-workers [Beckstein *et al.*, 2004]. Briefly, the grid dimensions containing the channel were 97×97×97 $Å^3$; a finer grid with dimension 10×10×10 $Å^3$ was used for focusing around the ion. The following parameters were used to simulate the environment: mobile ions Na^+ and Cl^- at a 0.150 M concentration; dielectric coefficients of 2.0 and 78 for the receptor and the solvent, respectively; temperature at 310 K. The electrostatic energy was calculated for three systems: $E_{protein}$, for the protein channel; $E_{ion}(z)$, for the ion by itself at each sample point *z*; $E_{complex}(z)$, for each protein-ion configuration (i.e. for each protein-ion complex with the ion at each sample point z). The PB energy at a sample point with coordinate *z* was then calculated, according to Tai *et al*. [2008], as:

$$\Delta E_{PB}(z) = E_{complex}(z) - E_{ion}(z) - E_{protein} \qquad \text{Eq (4)}$$

For visualisation of structures VMD [Humphrey *et al*., 1996] was used.

4.4 Extracellular Domain: Results

4.4.1 Long range: surface molecular electrostatics of the A and B subunits and AA, BB, AB and BA dimers

Electrostatics interactions are determinants since they are the driving forces for long range interactions and complex assembling. At short range, the effect of dispersion interactions (well represented by hydrophobicity and shape complementarity) becomes dominant to finely tune protein–protein association, while the role of electrostatics is that of providing key point of specific interaction on the surface. The molecular electrostatic potentials (MEPs) of the 5-HT_3R A and B extracellular subunits are shown in Figure 41. Here, the MEPs of both the principal and the complementary interface are depicted for subunits A and B. It is evident that while the principal interface of subunit A is mainly negative, its complementary side is mainly positive. In contrast, both the principal and the complementary interfaces of subunit B appear to be mainly negative. This MEP distribution has consequences on the types of dimers that can be assembled: the electrostatics will preferentially drive proteins with positive patches towards proteins with negative patches and vice versa. For example: the A complementary interface may interact with the A principal interface or with the B principal interface to form the AA dimer or the BA dimer respectively. This does not mean that only the AA and BA dimers can be formed but that those dimers are more probable to assemble than the others. The analysis of the MEP distribution on the dimer surfaces showed (Figure 41) that: dimer AA has a complementary interface which is positive and a principal one which is negative; dimer AB has a complementary interface which is positive and a principal interface which is negative, similarly to the AA dimer; the dimers BA and BB show a similar MEP distribution with both the complementary and the principal interfaces being mainly negative.

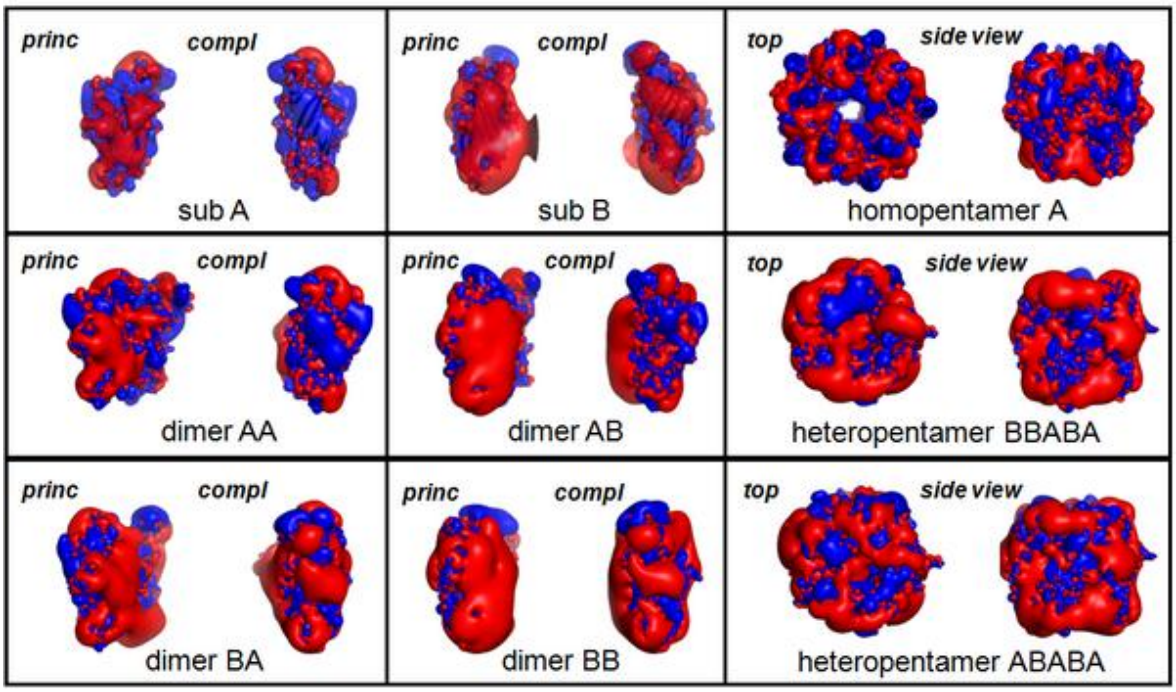

Figure 41– *Left):* Representation of MEP isocountour levels at +1 kT (blue) and -1 kT (red) of the principal and complementary interface of: *top* - 5-HT_3R subunits A and B; *middle and bottom* - 5-HT_3R dimers AA, BB, AB and BA. ***Right):*** MEP isocountour levels at +1 kT (blue) and -1 kT (red) of the side and top view of: *top* – 5-HT_3R homopentamer A; *middle* - 5-HT_3R heteropentamer BBABA; *bottom* – 5-HT_3R heteropentamer ABABA.

Finally, also the MEPs of three 5-HT_3R pentamers (Figure 41), i.e. the homopentamer A, the heteropentamer 3B : 2A (with a BBABA stoichiometry), the heteropentamer 3A : 2B (with a ABABA stoichiometry), are shown. Interestingly, the surfaces of the two heteropentamers appear highly similar and both their pores are highly negatively charged, as it would be required to transport a positive ion (Na^+ or Ca^{2+}). In contrast, the homopentamer A has a central pore which alternates positive and negative sites. This preliminary description is in agreement with previous experimental data showing that the single-channel conductance is higher in the heteropentamer AB than in the homopentamer A [Kelley *et al*., 2003; Hales *et al*., 2006; Peters *et al*., 2010].

4.4.2 Short range: physicochemical and structural analysis of the EC interfaces AA, AB, BA and BB

All the interfaces analysed are shape-complementary (their atom to atom distance ranges from 2.9 to 6.8 Å), therefore hereafter this index will not be analysed in detail, in fact the attention will be focussed on the description and analysis of the electrostatic potentials (EPs) and the hydrophobicities (H) of the dimer interfaces.

The interface AA. The electrostatic potential similarity index (EPSI) map shows that there is a high electrostatic complementarity in the core of the interface (Figure 42). In addition, in this area, the hydrophobicity similarity index (HSI) map shows that there are residues on both surfaces with similar hydrophobic properties (Figure 42).

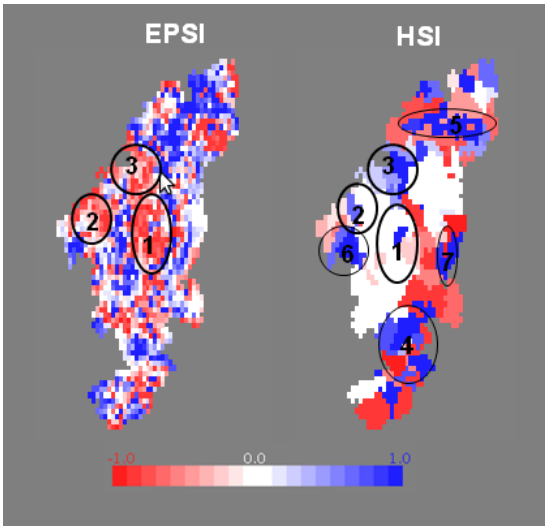

Figure 42- Homodimeric 5-HT_3R AA interface. *Left*- 2D maps of the electrostatic potential similarity (EPSI) of the principal subunit and the complementary subunit interfaces; *right*- 2D maps of the residue hydrophobicity similarity (HSI) of the principal subunit and the complementary subunit interfaces. EPSI ranges between -1 (red, complementary EPs) to +1 (blue, non complementary EPs); HSI ranges between -1 (red, non complementary hydrophobicities) to +1 (blue, complementary hydrophobicities). Maps were generated using the program MolSurfer [Gabdoulline *et al.*, 1999, 2003].

Three regions with very high complementary physicochemical features can be highlighted on the 2D surface:

Zone 1 (maximum value of EPSI in the area (max EPSI) = -0.999; HPSI = -0.365/+1): this region comprises the following residues: W178, L179 on the principal subunit; Y148, P150, W85 on the complementary subunit. It is a region rich in aromatic residues, which interact through an extended π–π stacking and originate an aromatic core. This was previously identified as the "hot core" [De Rienzo *et al*., 2012], i.e. the region responsible for the stabilization of the monomer–monomer interface. In addition, P150 has been previously demonstrated to be directly involved in receptor function [Moura Barbosa *et al*., 2010], therefore, it appears to be crucial (Figure 43).

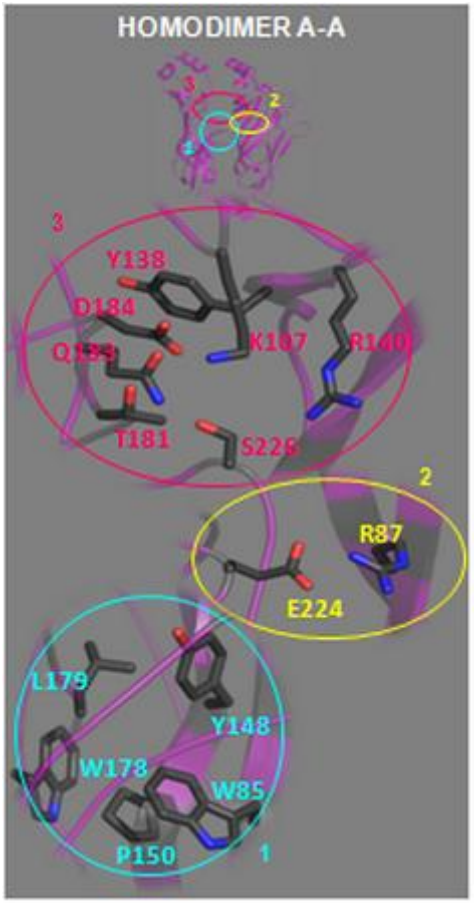

Figure 43- T*op* – Cartoon representation of the A-A dimer with the interface regions involved in interface stabilization highlighted; *bottom* – focus on Zones 1-3. Code for the cartoon representations: cyan: Zone 1; yellow: Zone 2; pink: Zone 3.

Zone 2 (max EPSI = -0.996; HPSI = -0.280/+0.7): this area is constituted by residue E224 on the principal subunit, and the interacting residue R87 on the complementary subunit: this is a charge-reinforced H-bond interaction, which keeps Loop C in the principal subunit bound to the complementary subunit. Such a clear electrostatic complementarity is complemented by a good hydrophobic complementarity (Figure 43).

Zone 3 (max EPSI = -0.975; HPSI = +0.280/+1): in this area, the following interacting residues are found: T181, Q183, D184, S226 on the principal subunit and K107, Y138, R140 on the complementary subunit. The principal surface is rich in negative and polar residues, while the second one is rich in positive and polar residues: both the electrostatic and hydrophobic complementarity criteria are satisfied (Figure 43).

As it can be clearly observed from Figure 42 bottom, at the AA interface there are additional areas showing complementary hydrophobicity (see for example, area numbers 4, 5, 6 and 7, where the HSI reaches values of about 1). This indicates that, once the two proteins have been brought into association distance, the binding is tuned by the presence of many local hydrophobic and dispersion interactions which are distributed over the whole interface surface.

The interface BB. The electrostatic complementarity of these two monomers is largely reduced with respect to the AA interface and it is not localised in a specific area of the interface. The hydrophobic complementarity instead is more preserved (Figure 44). This might suggest that should the two B subunits eventually come into contact (for example if forced by local spatial restraints), their association is then optimised and maintained by short-range interactions.

The "hot core" observed at the AA interface is completely missing at this interface: W178 in the principal subunit is substituted by His in the modelled structure of the B subunit [Moura Barbosa *et al.*, 2010] and by Ile in the 5-HT_3R subunit multiple sequence alignment (see alignment in Figure 39); the hot spot Y83 and Y68 in the complementary subunit are replaced by Ser and His, respectively; W85 in the complementary subunit is present although, in the 3D model, it interacts with E124 (on the principal subunit) instead that forming π-stacking interactions with other aromatic residues of the "hot aromatic core"; finally, Y148 is also present in the complementary surface, however it is not involved in the π-stacking interactions, which have been shown to be determinant for the interface stabilization in the A–A dimer.

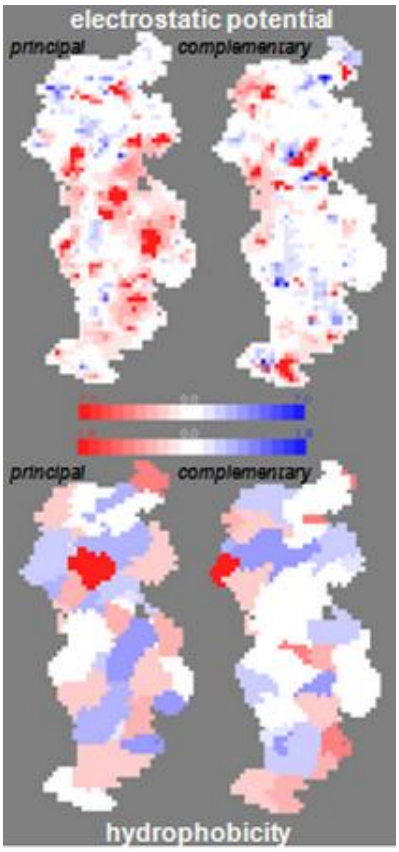

Figure 44- Homodimeric 5-HT_3R BB interface. T*op* - 2D maps of the electrostatic potential (EP) of the principal subunit and the complementary subunit interfaces; bottom - 2D maps of the residue hydrophobicity of the principal subunit and the complementary subunit interfaces. The electrostatic potential ranges from -7.0 Kcal/mol/e- (red; negative potential) to + 7.0 kcal/mol/e- (blue; positive potential); the hydrophobicity ranges from -1.8 kcal/mol (red, hydrophilic) to +1.8 kcal/mol (blue, hydrophobic).

The interface AB. This dimer is characterised by having an A monomer as the principal subunit and a B monomer as the complementary subunit. Interestingly, the physicochemical complementarity of the AB interface is intermediate with respect to that observed for the AA and that observed for the BB interfaces: it is largely reduced with respect to the AA interface and more extended than at the BB interface. The EP complementarity is displaced towards the dimer interface boundary, both in the region near the membrane and in the opposite region at the channel entrance, therefore, the residues determining the surface–surface complementarity are different from those in the AA system.

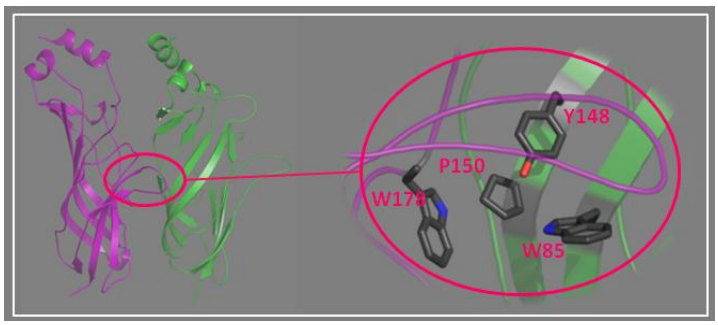

Figure 45- Heterodimeric 5-HT_3R AB interface: cartoon representation of the AB dimer with the residues constituting the "hot core" highlighted (focus on the right).

The unique interaction left from those constituting the AA "hot core" is between residue W178 in the principal subunit and P150 in the complementary subunit. In fact, the conserved residues W85, Y148 in the complementary subunit B are involved in the formation of other interactions with residues of Loop C (Figure 45).

The interface BA. This dimer is characterised by having a B monomer as the principal subunit and an A monomer as the complementary subunit. As highlighted in the previous cases, there are areas showing a good electrostatic potential complementarity, although the dimensions of these regions are largely reduced (i.e. they are formed by a lower number of residues) with respect to both the AA and the AB interfaces. These regions are also those showing the larger hydrophobic complementarity.

Of all the residues which have been shown to constitute the "hot centre" in the 5-HT_3R AA homodimer [De Rienzo *et al*., 2012], all those which are located at the complementary interface (i.e. Y68, Y83, W85 and Y148) are present also in the BA heterodimer, however they lack their counterpart on the principal subunit, the main hot spot W178 [De Rienzo *et al.*, 2012], which is here substituted by the His residue. This causes the loss of an aromatic cluster that forms the "hot core" and is centred at the aromatic residue W178 (in the principal subunit) of the AA interface with a consequent critical destabilization of the interface.

4.5 Extracellular Domain: Discussions

4.5.1 The 5-HT_3R assembling mechanism

In their recent work, Ortells and Barrantes [2008] have also tackled the problem of the assembly mechanism of the LGICs, by taking into account the various nAChR subunits. They tried to predict whether the β1δα1ɣα1 receptor assembles in a ‘‘heterodimer model’’ or in the alternative ‘‘sequential model’’. In the first case, the two dimers δα1 and ɣα1 form and then associate with each other and with the remaining β1 subunit; in the second case, heterodimers of different compositions are formed to assemble rapidly the α1β1ɣ trimer and subsequently add the δ and the second α1 subunits.

Determining the correct assembling mechanism of the 5-HT_3R is not straightforward. However, the analysis of the MEPs of the A and B subunits can help making some preliminary working hypotheses (to be further verified or confuted by experiments) about the reasonable and possible formation of dimers and of the final heteropentamers. On simple electrostatic bases, the dimers AA and BA appear to form with a higher probability than AB and BB. However, if also the hydrophobic and short range electrostatic interactions at the interface are considered, the AB interface seems to be more stable than the BA. In addition, the dimer AB appears to be the most reactive dimer since, having a positive complementary interface and a negative principal interface, it can interact with all other subunits or dimers. In contrast, the BA dimer, which has both the interfaces negatively charged, should interact preferably either with the A subunit or with the AB dimer, which both have a positive complementary interface.

Therefore, a few simple electrostatic-based mechanisms to assemble the pentameric receptors can be hypothesised:

(1) Five subunits A assemble one after the other to directly form the homopentameric receptor A or they assemble two by two, to form AA dimers which then assemble together and bind a fifth additional A subunit to get the receptor.

(2) Two AB dimers assemble to form an ABAB tetramer, which successively interact with either an A subunit to form an ABABA pentamer or with a B subunit to form a BBABA pentamer.

(3) A BA dimer assemble with an AB dimer to form a tetramer BAAB, which successively binds to a third A subunit to form an ABABA pentamer. In this case, the formation of a BBBAA pentamer seems to be less favoured, at least from simple electrostatic considerations.

4.5.2 Comparison of the 5-HT_3R interfaces

The analysis of the electrostatic and hydrophobic properties of the interfaces which can form the homo- and the heteropentameric 5-HT_3Rs confirmed the results of a previous study [De Rienzo *et al.*, 2012] based on computational alanine scanning, which highlighted the presence at the AA interface of a central aromatic region which stabilises the interface and therefore named the "hot core". This "hot core" and its local physicochemical complementarity is completely lost at the BB interface, where the local sequence and structure are different. Interestingly, the two heterodimeric interfaces, AB and BA, show properties which are intermediate between the two homomeric interfaces: at the AB interface, the "hot core" is partially maintained and the physicochemical complementarity in the corresponding area is also partially preserved. The maintained features are due to the presence of W178 in the A principal subunit. The BA interface instead is more similar to the BB one: although many residues forming the "hot core" are present on the complementary subunit (which is A subunit), they are not able to form a core aromatic cluster, probably due to the lack of the counterpart residue W178.

Thus, in agreement with the results previously found [Moura Barbosa *et al.*, 2010], the AB interface seems to be more similar to the AA one and the BA interface seems to be more similar to the BB one. According to the model based on the 2A:3B stoichiometry with a BBABA arrangement, the AB interface could apparently substitute the AA interface. This conclusion, although being in agreement with the hypothesis by Barrera and co-workers

[2005], disagrees with that of Lummis and co-workers [Lochner & Lummis 2010; Thompson *et al*., 2011]. Actually, these discrepancies among experiments and modelling studies could coexist in case that different cell types and/or different species express receptors with different stoichiometry or if the same interface in receptors with different compositions and stoichiometries assumes different conformations. A different explanation might be that the receptor behaviour does not depend only on the structure of its extracellular portion, but is instead due to other factors that are not taken into account here, which are connected either to the transmembrane or to the extracellular portion of the system. At present, more experimental information are needed to discriminate between the two principal hypotheses about the 5-HT_3R stoichiometry and assembly.

Previous works [Ortells & Barrantes, 2008] tried a superficial characterization of the 5-HT_3R interfaces AA, AB, BA and BB, and concluded that, while all these four dimers can form (at least from a shape complementarity point of view), the AA and BA interfaces should be characterised by stronger interface interactions than BB and AB.

These results are in partial disagreement with the results of the present study, which support a model where, although the formation of a BA interface appears to be favoured from the electrostatic point of view, the AB interface should behave more similarly to the AA interface. This discrepancy might be ascribed to the different 5-HT_3R structural models used: in fact, previous analyses [Ortells & Barrantes, 2008] were based on receptor monomers modelled using the AChBP structure as the template, while here the nAChR structure was used as the template, then pentameric receptor structures were assembled, optimised and used to extract dimeric models. It is also possible that the different conclusions are due to the different computational techniques used: here, the hydrophobic and electrostatic properties of dimeric couples are directly calculated, while previously [Ortells & Barrantes, 2008] property indices were computed which should be able to detect whether single monomer could or could not assemble into a dimer.

To get additional insights into this controversial issue, a much larger number of conformations of each dimer should be sampled and the physicochemical characterization repeated.

4.5.3 Comparison of the 5-HT_3R subunit sequences C, D and E

In the previous paragraph, the different interfaces found in the functional 5-HT_{3A}R and 5-HT_{3AB}R (with hypothetical stoichiometry BBABA) were analysed to compare their structural and physicochemical differences within the large structural and sequence composition of this class of receptors. This is nevertheless still a partial picture of the overall potential variability of the 5-HT_3R composition. In fact, besides the well characterised A and B subunits, at least three more subunits are found, named C, D and E, of which little is known. These other subunits could, at least in principle, form homomeric and heteromeric 5-HT_3R receptors. However, from experiments, it is known [Holbrook *et al.*, 2009] that, in order to be functional, subunits C, D, and E must be co-expressed with subunit A, therefore, no homomeric C, D, and E receptor will be considered hereafter.

Of course, further experimental work is required to verify if receptors with C, D or E subunits do exist and if they are active, however, in the meanwhile, it would be nevertheless interesting to try to predict whether heterodimeric 5-HT_3R extracellular interfaces containing monomers C, D and E could be functional or not. Here, a few hypotheses are worked out on the bases of the only information available about the receptor sequences and taking the moves from the above comparison performed on the interfaces containing subunits A and B. The interfaces formed by considering only binary heterodimers, i.e. 5-$HT_{3A/D}$R, 5-$HT_{3A/D}$R, 5-$HT_{3A/E}$R, are listed in Table 17.

Table 17- Amino acid residues at the interface of the homo- and hetero- 5-HT_3R interfaces and qualitative predictions on receptor functionality made on the basis of the information extracted from the computational model elaborated.

Dimer	Princ. Subunit	Residue Position 178	Compl. Subunit	Residue Position 68	83	85	148	150	Functional receptor prediction	References
A-A	A	**W**	A	**Y**	**Y**	**W**	**Y**	**P**	**yes**	[Moura Barbosa *et al.*, 2010; Jensen *et al.*, 2008]
B-B	B	H/I	B	H	S	W	Y	P	**no**	[Moura Barbosa *et al.*, 2010; Jensen *et al.*, 2008]
A-B	A	W	B	H	S	W	Y	P	maybe YES	
B-A	B	H/I	A	Y	Y	W	Y	P	probably NOT	
C-C	C	F	C	S	F	W	D	P	**NO from exp**	[Jensen *et al.*, 2008]
C-A	C	F	A	Y	Y	W	Y	P	maybe YES	
A-C	A	W	C	S	F	W	D	P	probably NOT	
D-D	D	S	D	S	-	-	K	T	**NO from exp**	[Jensen *et al.*, 2008]
D-A	D	S	A	Y	Y	W	Y	P	probably NOT	
A-D	A	W	D	S	-	-	K	T	probably NOT	
E-E	E	F	E	S	F	W	K	P	**NO from exp**	[Jensen *et al.*, 2008]
E-A	E	F	A	Y	Y	W	Y	P	maybe YES	
A-E	A	W	E	S	F	W	K	P	Probably NOT	

The next assumption is that, in order to be functional, the dimers formed by 5-HT_3R C to E monomers need to have similar physicochemical properties to those of the AA dimer. Therefore, the presence of the aromatic hot cluster, and in particular of residue W178 in the principal subunit and residues Y83, W85, Y68 and Y148 in the complementary subunit, will be taken as a reference point for functionality.

A further hypothesis is that an interface behaves always in the same way independently of the stoichiometry and composition of the receptor where it is found. For example, since the homopentamer 5-HT_{3B}R is not functional, each of its BB interfaces is supposed to be non-functional and therefore, also the BB interface found in the 5-HT_{3AB}R is considered to be non-functional. This assumption may of course be invalidated by significant conformational modification occurring in the heteropentamer, which are not present in the homomeric receptors.

The multiple sequence alignment reported in Figure 39 allows the comparison of the sequences A and B to the sequences C, D and E and the translation of the structural and physicochemical information from the first group to second group of sequences.

The first interesting observation is that, while C and E are highly similar (SeqI = 74%), D is different from all the other 5-HT_3R sequences, the most similar sequence being C with a SeqI of 42%. In fact, D shares only a 15% and a 21% sequence similarity with B and A, respectively: should D give origin to functional homo- or heteromeric receptors, we can expect these latter to have structural and functional determinants which are different from receptors composed of A and B subunits. W178, which is apparently a key feature of the AA interface, is not conserved in the 5-HT_3R D sequence, where at this position a Ser is located, which cannot maintain the aromatic interaction network formed by Trp (see Table 17).

At this same position (178), Phe is found in both 5-HT_3R subunits C and E: Phe may partially retain the properties of Trp and its capability of forming π–π stacking networks, while it has no capabilities of establishing polar interactions. W178 is not even present in the 5-HT_3R subunit B model, where it is structurally substituted by a His, which seems not to be able to maintain the interaction network of Trp, as showed by a recent Molecular Dynamics simulations study by De Rienzo and co-workers [2012]. In the multiple alignment of the 5-HT_3R subunit sequences, W178 of subunit A is substituted by Ile in subunit B: this residue is even less suited than His to keep the local aromatic network.

On the complementary surface, the hot spot Y83 (in the A subunit) [De Rienzo *et al.*, 2012] is substituted by Ser in the B subunit, which preserves only the polar features of Tyr, while both in C and E it is replaced by Phe, which potentially retains only the aromatic features of Tyr. Interestingly, in sequence D, position 83 is represented by a gap, which does not allow us to make any hypothesis about the protein structure in that region. While in all the other 5-HT_3R subunit sequences P150 is conserved, in subunit D it is substituted by a Thr: since P150 in subunit A is known to be determinant for the receptor functionality, its absence is a further hint of the incapability of this subunit D sequence to be functional.

The complementary subunit warm spot W85 [De Rienzo *et al.*, 2012] is conserved in all the sequences with the unique exception of 5-HT_3R D, where the sequence alignment shows the presence of a His, which is nevertheless polar and aromatic, although smaller than Trp. Position 68, which is occupied by Tyr in principal subunit A, is occupied by Ser in all the other sequences exception made for 5-HT_3R B, where it is a His. The common feature is the polarity, however only His retains the aromatic features of Tyr. Finally, residue Y148 in the complementary surface A is conserved only in subunit B, while it is replaced by Asp in sequence C and by Lys in both the D and E sequences. Both Asp and Lys can form H-bonds with nearby residues, but they destabilise the aromatic hot cluster. Substitution of Y148 at the AA interface with Lys would enlarge the positive electrostatic potential area on this zone in the complementary surface area, thus increasing the electrostatic complementarity, while the Asp would modify the electrostatic potential making it more negative and diminishing the local electrostatic complementary. In both cases (with Lys and Asp), the hydrophobic complementarity would be diminished. Mutations of this kind would reasonably modify the interface functionality, making it less active.

Thus, as it is summarised in Table 17, from this analysis based on the physicochemical properties of the interfaces and on previous CASM studies [De Rienzo *et al.*, 2012], only a few of the dimers studied should be functional. In particular, considering as fundamental the presence of Trp at position 178 at the principal interface and searching for the largest

similarities between the various interfaces and the AA interface, only the CA and EA interfaces appear to be able to build functional receptors: here, the complementary interfaces are the same as in the A–A dimer and W178 is replaced by a Phe, which can still stabilise the hot core π–π network.

Instead the AE and AC interfaces which have a complementary surface similar to the AA dimer (and a principal surface identical) will reasonably be non-functional (or at least less functional) due to the presence of a charged residue (Asp or Lys) which lowers the local surface–surface physicochemical complementarity. Similarly, also the homodimer EE and CC can be considered as non-functional interfaces. Finally, none of the dimers built by the 5-HT_3R D sequence appears to be functional, due to very different sequence of this monomer in the local interface area.

4.6 Transmembrane and Intracellular Domains: Results and Discussions

4.6.1 Modelling of the TM and IC domains of the 5-HT_3 A subunit

The model of the C-terminal part of the 5-HT_3A subunit is composed of four transmembrane α-helices (TM1, TM2, TM3 and TM4) and an intracellular α-helix (MA-helix). TM1 is connected to the EC domain and TM2 predominantly forms the wall of the channel pore (Figure 46a). A short intracellular loop connects TM1 to TM2 and a short extracellular loop connects TM2 to TM3. TM3 and TM4 are connected by a long intracellular segment, which the MA-helix belongs to. This region, with the exception of the MA-helix, has not been modelled here because of the lack of its atomic coordinates in the nAChR template [Unwin, 2005] (see Methods and Materials section). The 5-HT_3A subunit structure model is shown in Figure 46.

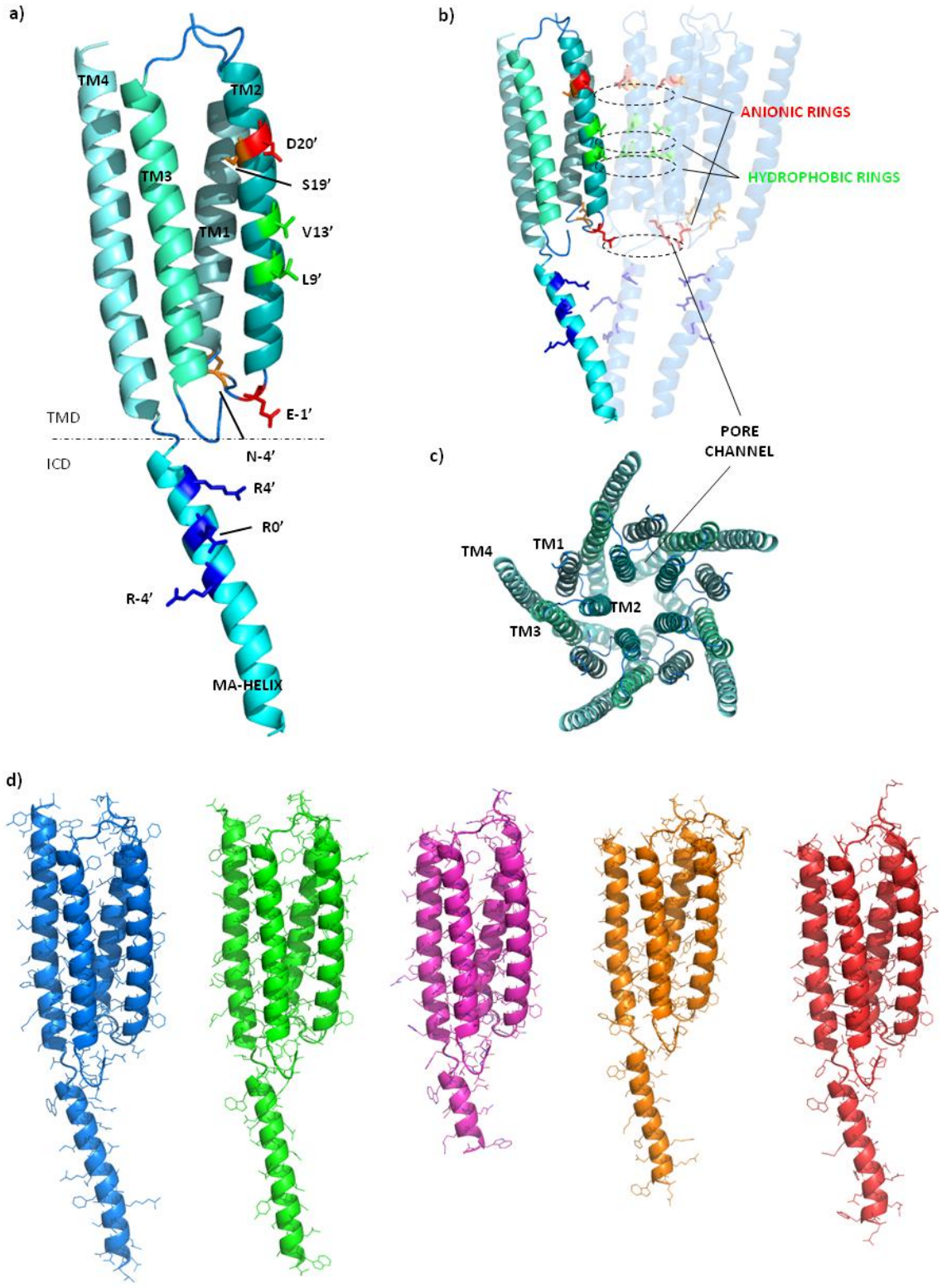

Figure 46 - a) Homology model of the TM and IC domains of the 5-HT_{3A}R subunit. The important residues for ion selectivity, conductivity and gating [Kienker *et al.*, 1994; Gunthorpe & Lummis, 2001; Thompson & Lummis, 2003; Yakel *et al.*, 1993; Paniker *et al.*, 2002; Dang *et al.*, 2000; Livesey *et al.*, 2008; Kelley *et al.*, 2003; Hales *et al.*, 2006; Peters *et al.*, 2010] are shown in sticks

and coloured according their physicochemical properties: basic amino acids are blue, acidic are red, polar are orange and non-polar are green. The prime numbering scheme for TM2 residues was described previously [Hales *et al*., 2006; Miller, 1989]. **b)** Homology model of three of the five 5-HT_3A subunits that compose the pentamer receptor, showing how the highlighted residues are able to form anionic (D20' and E-1') or hydrophobic (L9' and V13') rings around the pore channel. **c)** View of the homopentamer receptor 5-HT_3A from the extracellular side. The five subunits are assembled around a central channel pore and in each subunit the pore-lining domain consists of the TM2 transmembrane α-helix, while the TM1, TM3 and TM4 helices separate it from the membrane. **d)** Homology models of the five 5-HT_3R subunits: A, B, C, D and E.

The selected 3D model appears to be a good starting point for further analysis, since its overall geometry, stereochemistry and packing are is in compliance with the values typically observed in X-ray and NMR protein structures in the protein databases (see Materials and Methods section) and it describes correctly the available experimental information [Barnes *et al.,* 2009]. In particular, experimental site-direct mutagenesis data, performed either on the 5-HT_3R itself or on the nAChR, demonstrate the determinant functional role played by a few residues located in the TM2 and MA-helices (see Table 18): D-4' in the TM1-TM2 loop of nAChR; E-1', L9',V13', S19' and D20' in the TM2 helix; R-4', R0' and R4' in the MA helix.

Table 18- Single point mutations within the TM and IC domains, in particular within TM2 and MA-helix regions, of the 5-HT3A receptor or nAChR that affect functions.

Residue affecting function	Mutation(s)	Position	Receptor	Function(s) involved	References
D-4'	K	TM1-TM2 loop	nACh	Ion selectivity	Kienker *et al.*, 1994
E-1'	A	TM2	5-HT_3A	Ion selectivity, alone or combined with V13'T or S19'R	Gunthorpe & Lummis, 2001; Thompson & Lummis, 2003; Yakel *et al.*, 1993
L9'	F, Y, A, C	TM2	5-HT_3A	Channel gate	Paniker *et al.*, 2002
V13'	S, T	TM2	5-HT_3A	Channel gate; ion selectivity when combined with E-1'A	Gunthorpe & Lummis, 2001; Dang *et al.*, 2000
S19'	R	TM2	5-HT_3A	Ion selectivity when combined with E-1'A	Thompson & Lummis, 2003
D20'	A	TM2	5-HT_3A	Ion selectivity (reduced Ca^{2+} permeability)	Livesey *et al.*, 2008
R-4'	Q	MA-helix	5-HT_3A	Single channel conductance when combined with R0'D and R4'A	Kelley *et al.*, 2003; Hales *et al.*, 2006
R0'	D, E, Q, F, C	MA-helix	5-HT_3A	Single channel conductance, alone or combined with R-4'Q and R4'A	Kelley *et al.*, 2003; Hales *et al.*, 2006; Peters *et al.*, 2010
R4'	A	MA-helix	5-HT_3A	Single channel conductance, alone or combined with R0'D and R-4'Q	Kelley *et al.*, 2003; Hales *et al.*, 2006

By considering that these residues are involved in ion conduction and selectivity, it is reasonable to assume that they are oriented such as to be able to interact with ions passing inside the pore, i.e. their side chains protrude towards the centre of the channel. In the 3D model built for the 5-HT_3 subunit A, the relevant residues in Table 18 can be grouped as follows: group 1) consistently with the above assumptions, in the 3D model, the side chains of E-1', L9', V13', D20' in the TM2 helix, and R0', R4' in the MA helix are directed towards the receptor pore (Figure 46, a and b); group 2) residues S19' in the TM2 and R-4' in the MA-helix are not in contact with the pore channel (as clearly shown in Figure 46a and 46b), even though they are experimentally shown to be involved in ion selectivity and conductance; group 3) residue N-4', which is located in the TM1-TM2 linker and corresponds to the D-4' in the nAChR, does not protrude into the pore neither in the 3D model of the 5-HT_3R nor in the nAChR template, although it is known to be relevant for nAChR ion selectivity [Kienker *et al.*, 1994] (no direct information is instead available about its role in the 5-HT_3R) (Figure 46a). The static picture of the close state of the receptor given in this work cannot account for the dynamics of the channel and the concomitant rotation of TM2 which takes place during the activation process; therefore, a change in the conformation of the side chains of residues in group 2) can be envisaged.

4.6.2 Sequence and structure comparison of the 5-HT_3 A-E subunits

The TM and IC domains of the receptor subunits B, C, D and E share with the A subunit a sequence identity of 44, 46 39 and 48%, respectively, therefore they could reasonably be modelled directly onto the 3D model of the 5-HT_3R subunit A. The analysis of the sequence alignment and of the structural models obtained (Figures 40 and 46d) show that TM1, TM2 and TM3 are largely conserved within the 5-HT_3R subunits, while the TM4 is more variable. The major differences are found in the loops connecting the α-helices; in particular, the TM2-TM3 loop in subunit D is much longer than the corresponding loop in the other subunits and therefore it protrudes towards the extracellular portion of the receptor, where the long N-terminal domain (not included here) is found. In addition, the MA-helix in subunit C is shorter than MA-helices in the other subunits.

The modelled subunits A to E were combined to build 3D models of the 5-HT_3R TM and IC domains with different stoichiometries: 1) homopentameric 5-HT_3R A, B, C, D and E; 2) heteropentameric 5-HT_3R A/B with stoichiometries AAAAB, AAABB, AABBB, ABBBB, ABABA, BBABA; 3) heteropentameric 5-HT_3R A/C, A/D, A/E with stoichiometries analogous to the BBABA (i.e. CCACA, DDADA, EEAEA).

The analysis of the all these receptor models revealed that the intra- and inter-subunit interactions found are very similar among the different subunits. For example, a carbon-π network is found between few residues of TM1 and TM4 helices and is conserved in all the subunits (F264-I457, Y458-I261, Y265-L454 [sub. A numeration]; see Figure 47a); moreover, an inter-subunit carbon-π connects F14' (conserved in all the subunits) from TM2 to either I16' (A subunit), V16' (B subunit) or L16' (C, D and E subunits) from TM2 of the adjacent subunit (Figure 47b), which means that the same interaction is present between all subunit interfaces (AA, AB, BA, BB, AC, CC, CA, AD, etc...).

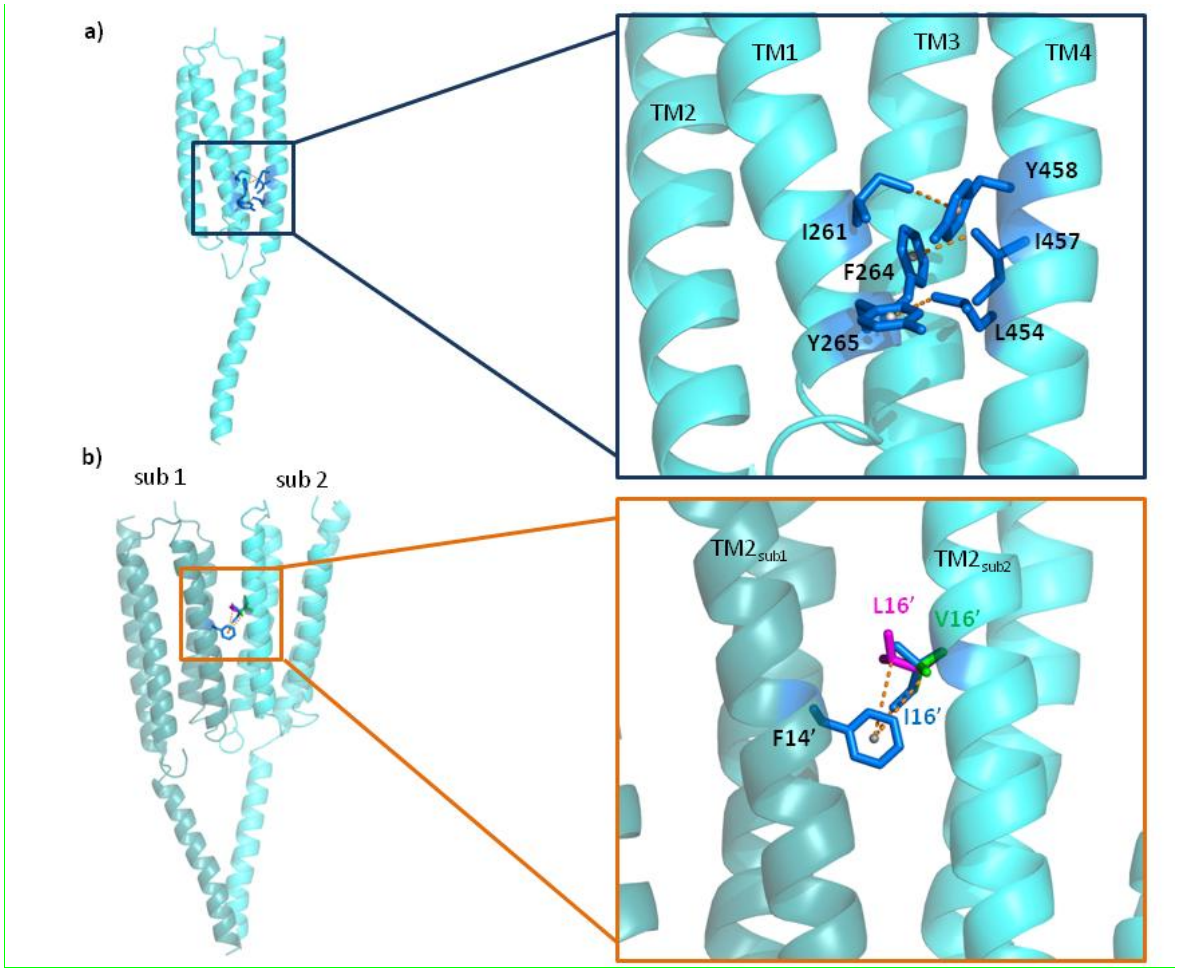

Figure 47- a) Homology model of the 5-HT_{3A}R subunit showing the intra-subunit carbon-π network found between few residues of TM1 and TM4 helices. This is conserved in all the subunits (F264-I457, Y458-I261, Y265-L454 [sub. A numeration]). **b)** Homology model of a dimer of the 5-HT_{3A}R showing the inter-subunit carbon-π that connects F14' (conserved in all the subunits, identified as sub 1) from TM2 to either I16' (blue, A subunit), V16' (green, B subunit) or L16' (pink, C, D and E subunits) from TM2 of the adjacent subunit (sub 2).

As for the relevant residues in Table 18, those at TM2 position 20', -1' and -4' were mutated in the nAChR [Kienker *et al.*, 1994; Corringer *et al.*, 1999] and were demonstrated to form three rings of residues along the pore that act as determinants of ion conduction in cation selective channel. The residues at positions 20' and -1', which are conserved in the 5-HT_3A subunit (Figure 40), have been shown to be determinant also in the 5-HT_3R [Gunthorpe & Lummis, 2001]. Gunthorpe and Lummis [2001] neutralised the intermediate ring of residues, inserted a Pro between the -1' and -2' residues [Cymes &

Grosman, 2011] and replaced the 13' Val by a Thr, transforming the cation permeable receptor into an anion permeable receptor. However, the single mutation of the E-1'A was proved to cause the channel to be non-selective [Thompson & Lummis, 2003]: this is a clear indication of the importance of this residue in controlling ion selectivity. Interestingly, this mutation is naturally present in the B subunit (the residue at position -1' is an Ala, instead of the Glu found in the A subunit; see Figure 40). This suggests that if the homomeric 5-HT_{3B}R was formed (as reported by Holbrook *et al.*, 2009, who observed the expression but not the function of the homomeric 5-HT_{3B}R), it would not be selective anyway. In subunit C, D and E the residue at position -1' is an Asn (Figure 40), which although not being charged, maintains the local physicochemical properties of subunit A, thanks to its polarity.

The negative ring formed by aspartic acids in position 20' is conserved in all the subunits, but the B subunit, where this position is occupied by an Asn (Figure 40), which is nevertheless polar. The absence of an acidic residue at the outer ring position of the β2 subunit of the nAChR has been demonstrated to cause a reduction in Ca^{2+} permeability [Tapia *et al*., 2007], as well as it happens in the heteromeric 5-HT_{3AB}R [Davies *et al.*, 1999].

As for residue at TM2 position -4', instead, sequences analysis pointed out that the properties of this residue, which is an Asp in nAChR α subunit, are conserved only in subunits C and D, where a Glu is present, while in the subunits A and B there is a polar residue (Asn), and in subunit E a positive one (Lys) (Figure 40). This variability causes the local properties of the different subunits to be largely diverse for the different 5-HT_3R subunits and suggests that the role of this residue might not be primary in the 5-HT_3 receptors. This hypothesis is supported by the fact that: 1) in analogy to the 3D structure of the nAChR, this residue is not protruding into the channel pore cavity of any of the modelled 5-HT_3Rs; 2) this residue has never been mutated in the 5-HT_3Rs, therefore its direct involvement in ion selectivity in the 5-HT_3R has not been directly ascertained, yet.

The key residues important for the conductivity (see Table 18) are those at the MA -4', 0' and 4' positions. In the 5-HT_3A subunit, these three residues, which lie at the boundary with the cytoplasmic region, are Arg. Site-directed mutagenesis experiments showed that

replacement of these three Arg, and in particular of R0', causes a large increase in channel conductance [Livesey *et al*., 2008; Hales *et al*., 2006]. These findings arose from the observation that the incorporation of the 5-HT_3B subunit (where no Arg is present at the key positions -4', 0', 4'; see Figure 40) into the receptor to form the heteromeric 5-HT_3AB makes the conductance increase, changing from values in the femtosiemens range (for the homomeric 5-HT_{3A}R) to picosiemens (for the heteromeric 5-HT_{3AB}R) [Davies *et al*., 1999]. The role played by R-4', R0' and R4' in modulating the receptor conductivity was confirmed also for the nACh α4β2 receptors, where the replacement of the natural residues at the MA -4' and 0' positions with Arg caused significant reduction of the single channel conductance [Hales *et al*., 2006]. Interestingly, in none of the other 5-HT_3R subunits (i.e. B, C, D and E) Arg residues are present at these sequence positions within the MA-helix, which are instead occupied by polar, negative or apolar residues: Q-4', D0', A4' in the B subunit; G-4', T0', E4' in the C subunit; E-4', Q0', E4' in the D and E subunits (see sequence alignment in Figure 40). This leads to the hypothesis that the heteropentamers 5-HT_3AC, 5-HT_3AD and 5-HT_3AE, by similarity with the 5-HT_3AB receptor, might have a larger conductivity than the homomeric 5-HT_{3A}R (note that single channel conductance of 5-HT_3AC, 5-HT_3AD and 5-HT_3AE heteromeric receptor has not been reported yet) [Walstab *et al*., 2012]. In contrast to the work of Holbrook and co-workers [Holbrook *et al*., 2009], where the alignment of the five 5-HT_3 subunit sequences showed a disruption of the 5-HT_3C MA-helix with residues at 0' and 4' positions not being represented, here the 5-HT_3C subunit model was built under the hypotheses that the MA-helix in the C subunit is shorter than in the other subunits, and that the key residues R-4', R0' and R4' in 5-HT_3A are replaced by Gly, Tyr and Glu, respectively, in the 5- HT_3A (Figure 40).

The last two noteworthy residues are the TM2 L9' and V13' in A subunit, which are supposed to be involved in the gate mechanism [Paniker *et al*., 2002]. In fact, experimental studies clearly demonstrated that the conserved L9' in TM2 domain plays an important role in gating: substitution of this amino acid with the more polar amino acid Thr affects the rate of desensitization and the EC_{50} for the activation of both the AChR and 5-HT_3R [Filatov & White, 1995; Yakel *et al.*, 1993]. In addition, the substitution

of V13' with a serine produces spontaneous gating in 5-HT_3R [Dang *et al.*, 2000]. MD simulations performed on nAChR showed that ligand binding induces the EC domain, and subsequently the TM domain, to rotate around the pore axis; in particular the twist centre seems to be the middle part of TM2, where the gate is probably located [Liu *et al.*, 2008] and where L9' and V13' are located. L9' and V13' are highly conserved among the 5-HT_3R subunits, the only exception being subunit B, where the conservative substitution L9'V is observed; thus, apparently, all the receptors studied should have the same gating mechanism.

In summary, a few determinant differences were found in the sequences and structures of the various subunits and receptors modelled: 1) in subunit B, the residue at the TM2 position -1, which is critical for ion selectivity, is an apolar Ala instead of a charged Glu or a polar Asn: this might alter the pore properties of the heteropentamer 5-HT_3AB (with the receptor stoichiometry modulating the ion selectivity) and might be among the reasons why the homomeric 5-HT_3R B does not assemble (it would be non functional anyway); 2) three Arg are found in the MA-helix of subunit A (R-4', R0' and R4'), which are lacking in all the other 5-HT_3R subunits, according to previous experimental data [Kelley *et al.*, 2003; Hales *et al.*, 2006; Peters *et al.*, 2010], which demonstrated that the presence of these Arg caused a lower single channel conductance in the A subunit with respect to the other subunits.

4.6.3 Electrostatic potential surface

The physicochemical characterization, and in particular the analysis of the electrostatic potential surfaces, of the TM and IC 5-HT_3R domains, is an interesting starting point to understand the different properties of the several pentamers forming the 5-HT_3R family.

The MEP isocontour levels are represented in Figures 48 and 50. The analysis of the electrostatic features was performed for the homopentameric receptors 5-HT_3A, 5-HT_3B, 5-HT_3C, 5-HT_3D and 5-HT_3E and of the heteropentameric receptors 5-HT_3AB, 5-HT_3AC, 5-HT_3AD and 5-HT_3AE with stoichiometry XXAXA (where X is subunits B, C, D or E). Only

for the most studied heteropentamer, the 5-HT_3AB receptor, all the other possible stoichiometries were also considered (ABBBB, AABBB, AAABB, AAAAB, ABABA).

5-HT_3A homopentamer receptor surface. The first evident feature shown by the TM and IC domains of the homopentamer 5-HT_{3A}R is the overall negative electrostatic potential inside the pore (Figure 48a). Smaller regions of positive potential are located at the upper region of the TM domain, where the EC domain is located (Figure 48a). To this respect, the electrostatic potential of the region at the boundary between the EC and the TM domains might suffer from the fact that the EC domain is not included in the models. Examination of the pore model structure of 5-HT_{3A}R shows that the majority of the TM2 residues forming the pore are negatively charged or at least polar residues, such as Asp, Glu, Thr or Ser, which give the pore its negative potential. The portion of the IC domain closer to the membrane is also characterised by a negative potential (see Figure 48a), despite the presence of three Arg (R-4', R0',R4') in the amino acid sequence (see Figures 40 and 46a).

The large negative potential along the TM channel and part of the IC channel is likely to play a significant role in the interaction of the receptor with ions. In fact, previous studies demonstrated that there is a very high barrier for an ion moving inside a low dielectric environment [Parsegian, 1969; Partenskii & Jordan, 1992], suggesting, therefore, that ion channels (which represent a low dielectric environment) need charged surfaces, or at least partial charged surfaces, in order to allow ions to enter. This hypothesis was subsequently investigated and confirmed by Kuyucak *et al*. [1998], who analysed the interaction of ions with a simple geometry channel.

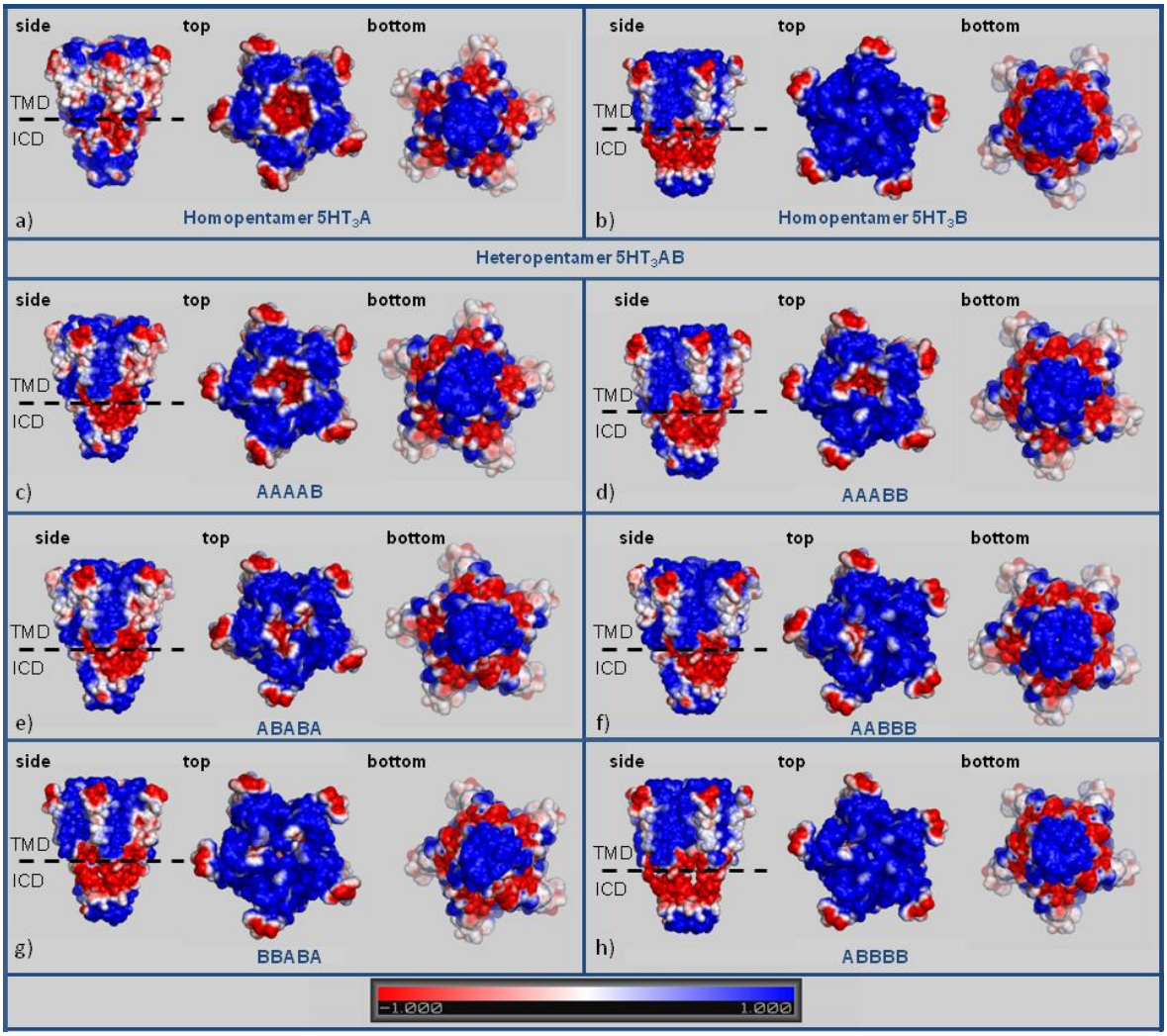

Figure 48- Electrostatic properties of the homomeric and heteromeric 5-HT_3A, 5-HT_3B and 5-HT_3AB receptors. MEP isocontour levels are shown at +1 kT/e (blue) and −1 kT/e (red). ***a):*** Representation of MEP isocountour levels of the side, top and bottom view of homopentamer 5-HT_3A; ***b):*** Representation of MEP isocountour levels of the side, top and bottom view of homopentamer 5-HT_3B; ***c-h):*** Representation of MEP isocountour levels of the side, top and bottom view of all the stoichiometries of heteropentamer 5-HT_3AB.

On the contrary, the C-terminus of the IC domain (i.e. the region more distant from the membrane) is characterised by a large area of positive potential that, on simple electrostatic consideration, repels the cation, promoting its exit through the lateral openings (portals) found in the receptor IC domain (Figure 48a).

These portals are formed at the interface of two adjacent MA-helices and are therefore five. Interestingly, they show surface electrostatic potential that is overall negative and could in fact attract the cations. The presence of highly charged portals, through which ions go out of the channel, was previously suggested by Mokrab and co-workers [Mokrab *et al.*, 2007] for the GABA receptor, which is anion-selective; in that work, the interaction energy between a Cl^- ion and the GABA model structure was calculated along the central pore of both the EC and TM domain, and along the putative exit paths in the IC domain through each of the five portals, to determine the most favourable energy profiles.

The five portals in the 5-HT_3A homopentamer are not completely negatively charged (see Figure 49) and show instead local areas of positive potential. The presence of these positive spots could slow down the movement of cations though the portals and thus explain the lower single channel conductance observed for the homopentamer A with respect to the heteropentamer AB. The positive areas inside the portals are due to the three non conserved Arg located in the TM2 (R-4', R0',R4') [Hales *et al.*, 2006], whose role has been discussed in a previous paragraph.

5-HT_3B homopentamer receptor surface. The electrostatic potential map of 5-HT_3B homopentamer receptor surface reveals in part opposite characteristics with respect to those of the 5-HT_3A homopentameric receptor. The TM domain of the 5-HT_3B homopentameric receptor has a positive MEP, both inside the pore and outside, with very small regions of negative potential in the external part of the receptor, near the EC domain (Figure 48b). On the contrary, with the exception of the positive potential of the MA-helix N-terminus (which lies far from the membrane), the IC domain is characterised by an overall large negative electrostatic potential.

Interestingly, the MEP that characterises the TM domain channel in the homopentameric 5-HT_{3B}R, is highly positive, despite the low number of positive residues in the TM2 sequence (Figure 40). This is due to the fact that the two important negative residues E-1' and D20' which were found in the A subunit TM2, are substituted in the B subunit by non-charged residues (i.e. E-1'A and D20'N). This is a further confirmation of the role played in ion selectivity of the two charged rings formed by these residues in the TM2 helix bundle

of the receptor (-1' and 20'; see Modelling section) [Gunthorpe & Lummis, 2001; Thompson & Lummis, 2003].

5-HT$_3$AB heteropentameric receptor surface. Surprisingly, the potential surface map of the heteropentameric 5-HT$_3$AB receptor, with the stoichiometry BBABA proposed by Barrera and co-workers [Barrera et al., 2005], exhibits the same qualitative electrostatic characteristics of the homopentamer 5-HT$_{3B}$R, i.e. a positive pore surface in the TM domain, a negative surface at the entrance of the ICD (near the membrane), and a positive region at the N-terminus of the MA-helices (Figure 48g). Such a MEP similarity suggests that also the heteromeric BBABA receptor could be non functional, as well as the homomeric B pentamer. Similarly, the analysis of the MEPs of the heteropentameric 5-HT$_{3AB}$R with other stoichiometries such as AABBB, or ABBBB, shows that the presence of three or more B subunits confers upon the pore a positive potential that could disadvantage or block the cations passage (Figure 48f and 48h), due to electrostatic repulsion. However, it is worth noting that, as it has been showed in the previous paragraphs, the MEP of the BBABA EC portion is highly negative, and therefore seems to be favourable to cation permeation. The fact that the pore has electrostatic features in the EC and TM domains which are almost opposite might have relevant implications for the effective functionality of the 5-HT$_3$R with this stoichiometry: it cannot be excluded that this receptor is functional notwithstanding the TM domain pore electrostatics.

On the contrary, in pentamers with stoichiometry 2B:3A and 1B:4A (i.e. AAAAB, AAABB or ABABA), the pore potential surface is mainly negative (Figure 48c, d and e): in these cases the A subunit characteristics prevail, giving to the system properties similar to those of the homopentameric 5-HT$_{3A}$R TM and IC domains. Interestingly, the EC pore MEP of the ABABA receptor is negative (see the Extracellular Domain section), thus the whole receptor pore (the EC, the TM and the C-terminal IC domains pore) is completely negative, with the only exception of the MA-helix N-terminus (Figure 48e). Therefore, on simple electrostatic bases, of all the possible receptor stoichiometries considered here, the one which seems to be fully functional is the heteropentamer ABABA, followed by the homomeric A, although functionality cannot be excluded also for the heteromeric BBABA.

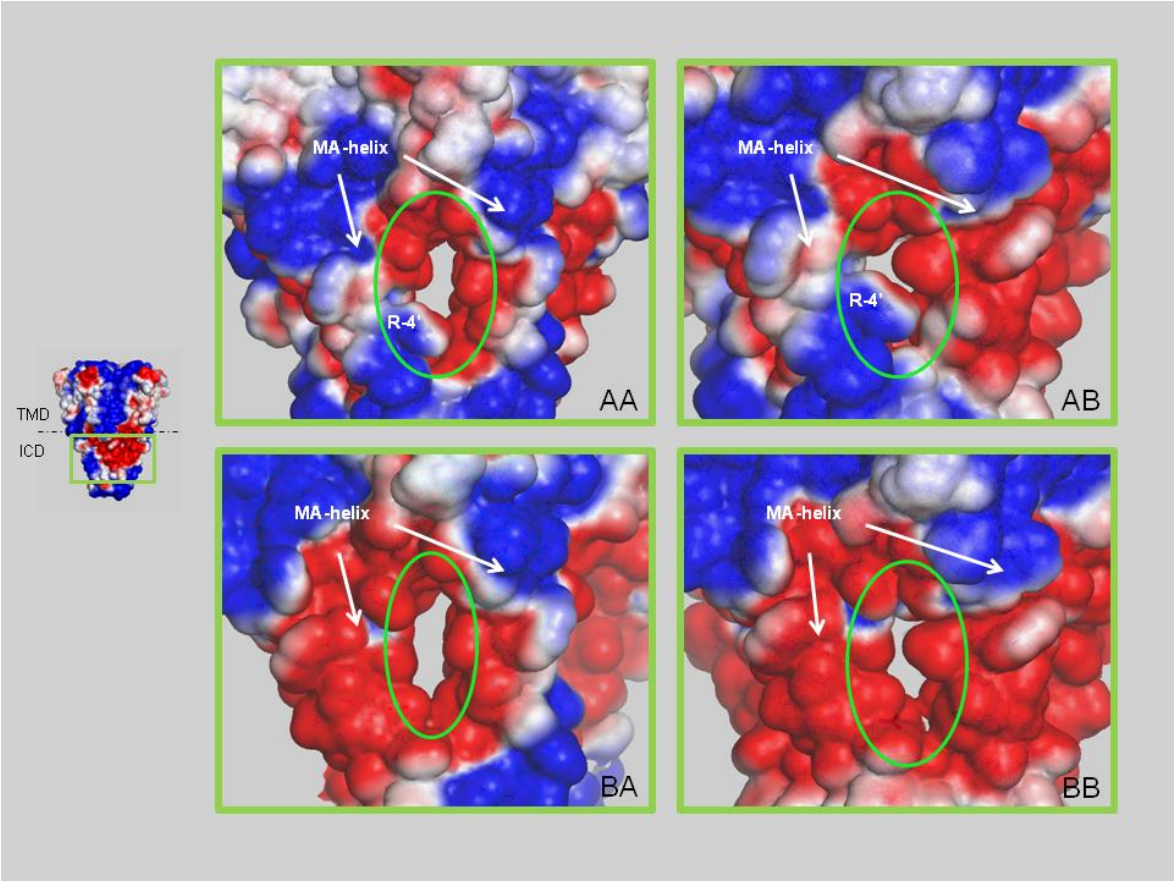

Figure 49- Electrostatic properties of the portals in the 5-HT_{3AB}Rs IC domain, probably way out of ions. MEP isocontour levels of exterior views of the IC domain section are shown at +1 kT/e (blue) and −1 kT/e (red) for AA, AB, BA and BB portals, formed between two adjacent MA-helices.

The IC domains of the various receptors built differ mainly in the region of the portals formed between two adjacent MA-helices; in fact, portals formed by different subunits (AA, AB, BA, BB) show different dimensions and potentials (Figure 49). More precisely, the BB and BA portals are the largest and completely negative, the AA portal is smaller than the BB and BA portals and has a positive MEP region due to the presence of R-4', R0' and R4' in the A subunit, and, finally, the AB portal is the smallest and has a MEP distribution which is similar to that of the homopentamer A portal. The different features of the portals could influence the ion exit in different manners, increasing the single channel conductance when at least a B subunit is present, in agreement with the experimental data [Hales *et al.*, 2006].

In summary, the heteropentamer 5-HT_{3AB}R with BBABA stoichiometry [Barrera *et al.*, 2005] seems to have a TM domain pore MEP that does not favour the cations passage, being positive, although the EC pore portion, which is instead highly negative, seems to promote cation passage. The receptor stoichiometries that have a negative TM domain pore potential surface, which could attract cations, are AAABB, AAAAB and ABABA. These results seem to support the hypothesis by Lochner and Lummis [Lochner & Lummis, 2010] according to which the BBABA stoichiometry is not functional, because it lacks the minimum requirements of an interface AA. From the analysis of the electrostatic surface properties of homopentameric 5-HT_3A and 5-HT_3B and heteropentameric 5-HT_3AB receptors performed in this work, having at least an AA interface is not the unique requirements for the receptor to be functional. In fact, the pentamer AABBB, containing an AA interface, presents a positive surface along the TM pore, which may prevent or limit the cations passage; the analysis of the electrostatic potential at surface suggested that also a maximum of two B subunits favours the receptor functionality. Of course, other and more sophisticated analyses might provide additional information and demonstrate that functionality is not simply related to electrostatics.

5-HT_3C, 5-HT_3D, 5-HT_3E homopentameric receptor surfaces. Figure 50 (*left)* shows the potential map surfaces of the homopentameric 5-HT_3C, 5-HT_3D and 5-HT_3E receptors which exhibit very similar characteristics to the homopentamer 5-HT_3A receptor. In fact, the pore surface is characterised in all cases by a negative MEP, extending from the TM domain near the EC domain until the centre of the MA-helix in the IC domain, while the IC domain C-terminus is on the contrary positive.

There is still an open debate on the expression of the homopentamer 5-HT_3C, 5-HT_3D and 5-HT_3E receptors: Nielser and co-workers [Nielser *et al.*, 2007] have shown that subunits C, D and E do not reach the plasma membrane unless co-expressed with the A subunit, while Holbrook and co-workers [Holbrook *et al.*, 2009] suggest that these subunits can independently reach the plasma membrane. However, both the studies agree on the non-functionality of these three homopentamers. Considering the results obtained in this

work, it is not possible to find a reasonable explanation to their lack of functionality, which is probably due to factors diverse from those analysed here.

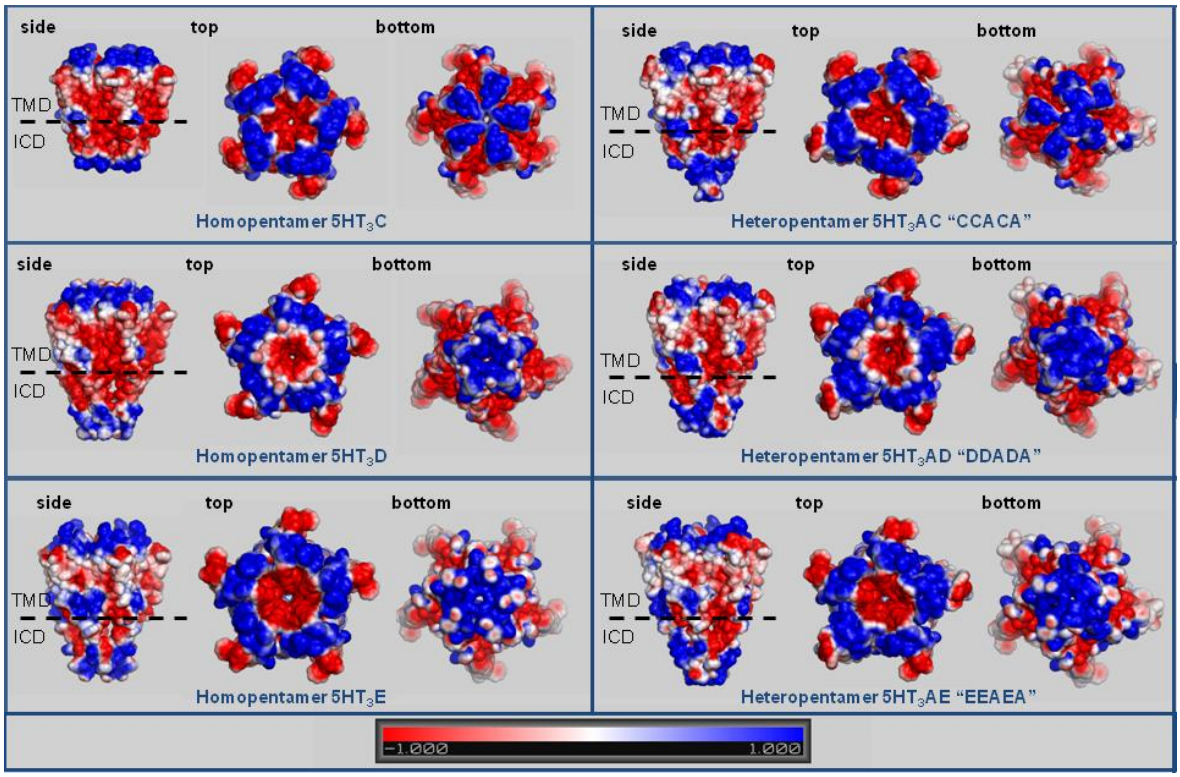

Figure 50- Electrostatic properties of the homomeric 5-HT_3C, 5-HT_3D, 5-HT_3E and heteromeric 5-HT_3AC, 5-HT_3AD, 5-HT_3AE receptors. MEP isocontour levels are shown at +1 kT/e (blue) and −1 kT/e (red). ***Left)****:* Representation of MEP isocountour levels of the side, top and bottom view of homopentamers 5-HT_3C (*top*), 5-HT_3D (*middle*) and 5-HT_3E (*bottom*); **right)***:* Representation of MEP isocountour levels of the side, top and bottom view of heteropentamers 5-HT_3AC (*top*), 5-HT_3AD (*middle*) and 5-HT_3AE (*bottom*).

5-HT_3AC, 5-HT_3AD, 5-HT_3AE heteropentameric receptor surfaces. For 5-HT_3R subunits C, D and E, only the heteropentamers with stoichiometry similar to that experimentally found for the B subunit [Barrera *et al.*, 2005] (CCACA, DDADA, EEAEA) have been taken into account. The potential surface maps of the heteropentameric 5-HT_3AC, 5-HT_3AD and 5-HT_3AE receptors are not different from those of the corresponding homopentameric receptors: a negative MEP prevails along the pore (Figure 50 *right*), which might attract cations, promote their passage and force them to exit through the large and negative portals. The single channel conductance, which has not been experimentally measured

yet [Walstab et al., 2010], should be greater in the heteropentameric 5-HT_3AC, 5-HT_3AD and 5-HT_3AE receptors than in the homopentamer 5-HT_{3A}R. However, further hypotheses about the putative stoichiometry of these three heteropentamers cannot be developed on simple electrostatic characteristics, since their MEPs are highly similar to that of the homopentamer 5-HT_{3A}R.

4.6.4 Pore Profile

On the basis of the results obtained by MEP analysis, the homopentameric and heteropentameric receptors built by subunits A and B were selected for a deep characterization of the physicochemical properties of their pores.

It is important to remember that these models should correspond to a closed state of the channel, because the structure of the templates was obtained in absence of the agonist and corresponds to a closed conformation.

Analysis of the 5-HT_{3A}R pore radius profile (Figure 51b) showed that there are some constrictions along the length of the pore, which extends along the z axis, from z ~ 56 Å (TM domain portion at the IC boundary) to z ~ 103 Å (TM domain portion at the EC boundary). At the smallest section of the channel, which is in the proximity of the TM2 T6' ring and of the hypothesised gate channel formed by L9' and V13' [Yakel *et al.*, 1993; Paniker *et al.*, 2002; Dang *et al.*, 2000], the channel radius decreases to about 3 Å; another narrowing, where the channel radius is about 3.5 Å, is in the nearby of the TM2 E20' ring of residues, which is important for the ion selectivity [Gunthorpe & Lummis, 2001; Thompson & Lummis, 2003], as previously discussed. These results are consistent with those obtained for the nACh receptor in previous studies [Amiri *et al.*, 2005], where it was suggested that the conserved rings of L9' and V13' do not form a physical block in this region, but constitute an ion-impermeable hydrophobic barrier [Miyazawa *et al.,* 2003]. More in detail, Beckstein and co-workers [Beckstein & Sansom, 2006] explain that a hydrophobic gate acts as a desolvation barrier for ions, in fact the narrow pore radius

(R < 4 Å) forces ions to shed at least some water molecules from their hydration shell, which requires a large amount of energy, in order to pass the constriction.

In addition to the pore radius profile, the energetic profile of a Ca^{2+} ion, as it translates along the pore axis, has been estimated by means of Poisson-Boltzmann energy calculation. This method has some intrinsic limitations such as: static protein structures are considered and only the long-range electrostatic forces are calculated, therefore the non-electrostatic effects and those due to movements of the pore-lining residues are not considered. To include these effects, energy profiles could be computed by potential mean force (PMF) calculations, which are based on molecular dynamics. These calculations would be more accurate, but at the same time much more time-expensive. Previous studies [Beckstein *et al*., 2004] demonstrated that, notwithstanding PB calculations commonly overestimate the barrier for narrow (<3 Å) channels with respect to PMF calculations, the two methods reach the same conclusions [Amiri *et al*., 2005].

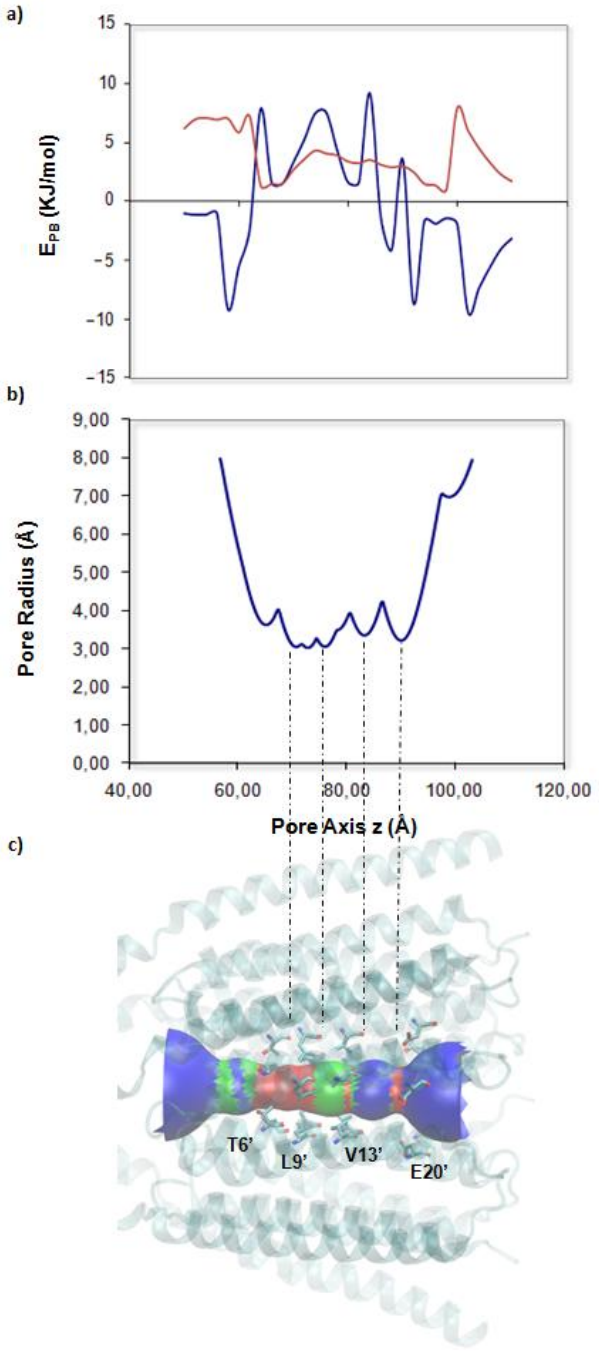

Figure 51- ***a)*** PB energy profiles for a calcium ion (blue line) and a chloride ion (red line) encountering the 5-HT_{3A}R pore; ***b)*** pore radius profile for the 5-HT_{3A}R pore; ***c)*** model of the 5-HT_{3A}R oriented such that the pore (*z*) axis coincides with that of the graphs a) and b) (to the left is the IC domain, right, the EC domain; neither shown). The solid surface in c) represents the pore lining surface, calculated using HOLE [Smart *et al.*, 1996] and coloured on the basis of the radius pore as follows: R < 3.5 Å red, 3.5 Å < R > 4 Å green, R > 4 Å blue. Residues of interest, corresponding to the constrictions of the pore lining surface, are shown in sticks. Note that these residues match to the minima in the pore radius pore (b) and to the peaks on the calcium ion PB energy profile (a).

The plot in Figure 51 a shows the PB energy profile of a calcium ion approaching the 5-HT_{3A}R channel from the extracellular domain (right). At the beginning, the ion encounters a favourable attraction, probably due to the negative potential that characterises the pore (see Electrostatic potential surface section). Then, it encounters first a moderate energy barrier at z~ 90 Å, where the first narrowing of the pore is located (corresponding to residue E20'), and subsequently a larger barrier, in the centre of the pore. The latter extends from the V13' through the L9' to the T6' side chain rings, where the peaks of the barrier (~ 9 KJ/mol) are located, thus providing a significant block to permeation and confirming that the model of the channel corresponds to a closed state, as it was expected.

At the end of the TM domain, towards the IC domain, the PB energy becomes negative again. These results are again consistent with those obtained for the nACh receptor [Miyazawa *et al*., 2003; Amiri *et al.*, 2005] and with the hypothesis of a hydrophobic gate, formed by a hydrophobic region in the centre of the pore [Paniker *et al.*, 2002] that plays a role as a barrier to ion permeation in the closed receptor conformation.

For comparison, the PB energy profile of the Cl^- ion has also been calculated. The energy profile showed in Figure 51 a reveals a totally non favourable permeation of this anion through the 5-HT_{3A}R pore. In particular, chloride ions encounter a high barrier (~ 7 Å) already at the channel entrance. This repulsion is probably caused by a Glu in TM2 position 20' (whose structural position corresponds to the peak barrier). This demonstrates that the presence of this negative residues at the TM channel entrance, together the whole negative pore MEP in the TM domain, contributes to the ion selectivity of the channel.

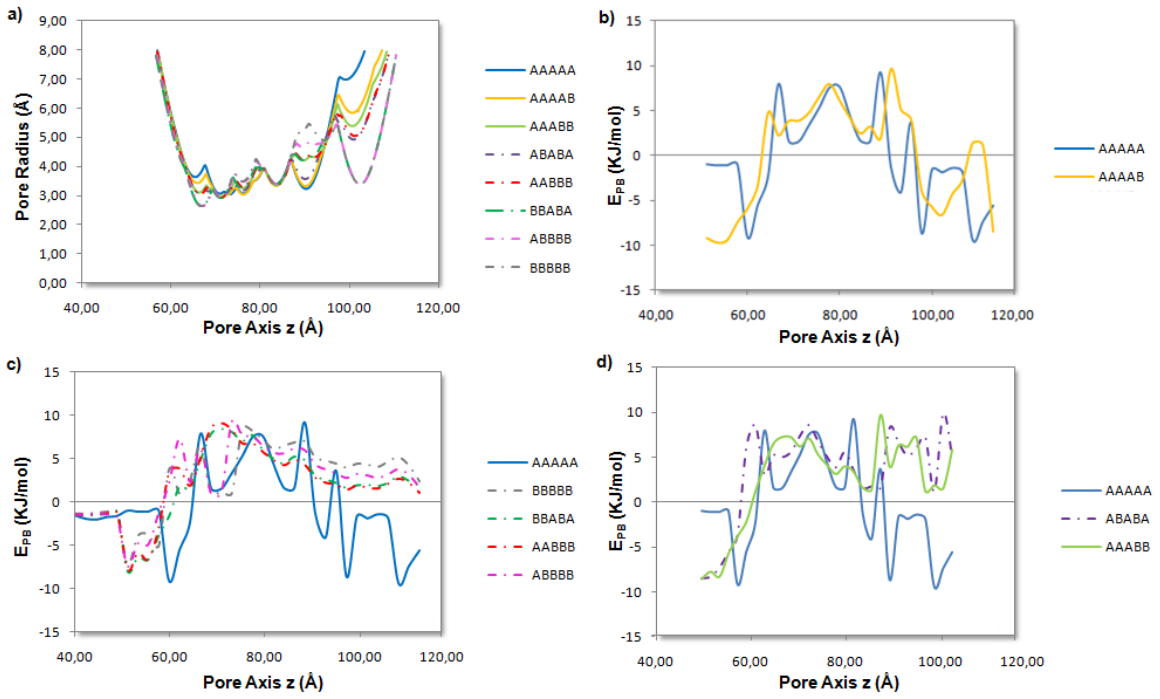

Figure 52- Pore radius profiles (a) and calcium ion PB energy profiles (b, c, d) for homomeric and heteromeric 5-HT_3A, 5-HT_3B and 5-HT_3AB receptors: 5-HT_{3A}R "AAAAA" in blue, 5-HT_{3B}R "BBBBB" in grey (dashed line), 5-HT_{3AB}R "AAAAB" in yellow, 5-HT_{3AB}R "AAABB" in green, 5-HT_{3AB}R "ABABA" in purple (dashed line), 5-HT_{3AB}R "AABBB" in red (dashed line), 5-HT_{3AB}R "BBABA" in deep green (dashed line), 5-HT_{3AB}R "ABBBB" in pink (dashed line).

The pore radius and the PB energy profiles of the homopentamer 5-HT_{3B}R and of the various stoichiometries of the heteropentamer 5-HT_{3AB}Rs have been analysed and compared to those of the homopentamer 5-HT_{3A}R. The pore radius profiles (Figure 52a) show similar trends at the level of the channel gate (V13', L9') and of the T6' residue ring, and the main differences with the homopentamer 5-HT_{3A}R are located in three principal regions:

- at z~ 101 Å: in the A subunit is present an Ala, whereas in the B subunit there is a bulkier Arg. There, the radius decreases with the increasing of the number of B subunits present in the receptor (i.e. radius 5-HT_{3A}R = 7 Å vs radius 5-HT_{3B}R = 3.5 Å), and, in case the number of B subunits in the receptor is the same, the local channel radius is smaller where B subunits are not adjacent;

- at z ~ 90 Å: in the B subunit is present an Asn instead of the Asp of the A subunit. There, the radius increases with the increasing of the number of B subunits present in the receptor (i.e. radius 5-HT_{3A}R = 3.5 Å vs radius 5-HT_{3B}R = 5.3 Å);

- at z ~ 65 Å: in the B subunit is present an Ile instead of the Val of the A subunit. There, the radius decreases with the increasing of the number of B subunits present in the receptor (i.e. radius 5-HT_{3A}R = 4 Å vs radius 5-HT_{3B}R = 2.7 Å).

Analysing the trend of the PB energies of the homopentamer 5-HT_{3B}R and of the heteropentamer 5-HT_{3AB}Rs, it is possible to distinguish three different profile types. The first type is that of the "AAAAB" heteropentamer, which is very similar to that of the homopentamer 5-HT_{3A}R (Figure 52b), characterised by the same peak in correspondence of the channel gate. The only difference is a small peak (1.20 KJ/mol) present at the beginning of the pore, which corresponds to the Arg294 in the B subunit (here, the potential is positive and the radius of the pore smaller). The second profile type groups together the homopentamer 5-HT_{3B}R and the "ABBBB", "AABBB" and "BBABA" heteropentamers. These receptors have in common a positive pore surface potential (see Electrostatic potential surface section), that is consistent with a non favourable PB energy profile showed in Figure 52c. The peaks are in the same regions of those of the homopentamer 5-HT_{3A}R and the "AAAAB" heteropentamer, but have a major intensity, which increases with the number of B subunits. This type of profile, similar to that of the chloride ion through the 5-HT_{3A}R, suggests the presence of a high energy barrier that contrasts the cations passage through the pore, and confirms the results obtained from the analysis of the MEPs (see Electrostatic potential surface section). Finally, the third profile type groups the last two heteropentamers, "ABABA" and "AAABB", which are characterised by a negative pore surface MEP (see Electrostatic potential surface section) and for which it was expected a PB energy profile not too different from that of the homopentamer 5-HT_{3A}R or that of the "AAAAB" heteropentamer. Differently from what expected, their PB energy profiles are quite anomalous: they show a series of peaks, in

particular at the channel entrance, that are not presents in the PB energy profiles of the other receptors (Figure 52d). Furthermore, what was mainly unexpected is the totally unfavourable interaction energy profile, which is difficult to explain given the negative pore MEP of the "ABABA" and "AAABB" heteropentamers. The calcium ion should encounter a favourable attraction while entering the channel; conversely, it seems to be repelled by the channel in these two receptors, as testified by the several energetic barriers it encounters. Thus, further analyses of these receptors seem to be necessary to clarify the unexpected behaviour of the "ABABA" and "AAABB" heteropentamers. Probably, in this case, the limitations of the PB method become important and prevent a correct interpretation and analysis of the receptors features, and/or the presence of the EC domain receptor structure, not considered in this work, exerts important modifications of both the structure and the electrostatic properties of the TM domain.

In summary, it has been shown that the hydrophobic belt at the centre of the 5-HT_3R pore acts as a hydrophobic gate, increasing the energy barrier encountered by a putative calcium ion moving through the channel. Moreover, the homopentamer 5-HT_{3A}R and the heteropentamer 5-HT_{3AB}R with stoichiometry "AAAAB" have very similar PB energy profiles, which are consistent with the MEP features and with the experimental results on 5-HT_3R [Gunthorpe & Lummis, 2001; Thompson & Lummis, 2003; Paniker *et al*., 2002] and on nAChR [Miyazawa *et al*., 2003; Amiri *et al*., 2005]. The homopentamer 5-HT_{3B}R and the heteropentamer 5-HT_{3AB}Rs with the stoichiometries "ABBBB", "AABBB" and "BBABA" share a similar PB energy profile, which is not favourable to the cations passage, suggesting that these receptors are non-functional and confirming the results obtained from the MEP analysis. Finally, for the heteropentamer 5-HT_{3AB}Rs with stoichiometries "ABABA" and "AAABB", further analysis are required to understand their unexpected behaviour.

4.7 Conclusions and Perspectives

The long-range interaction features of the ECD of subunits 5-HT_3R A and B and of their possible combinations into dimers are analysed together with the physicochemical properties both of the various putative EC 5-HT_3R interfaces (on the bases of the structural conformations of the models and of the known sequences) and of the TM and IC domains of the 5-HT_3 receptor family, in order to develop working hypotheses about the stoichiometries and functionalities of the receptors.

The results for the ECD confirmed the presence of an aromatic cluster, located in the core of the AA interface, as the key determinant of the monomer–monomer stability, in agreement with previous studies. This cluster is completely absent in the BB dimer which is known to give origin to non-functional homopentameric 5-HT_3Rs. On this basis, among all the other possible interfaces constituted by the known 5-HT_3R sequences A, B, C, D, and E, only the CA and EA interfaces are predicted to be able to build functional receptors.

Two major structural differences are highlighted by the analyses of the amino acids sequence and 3D structure of the five modelled TM-IC domain subunits (5-HT_3 A to E): i) subunit B might be ion-unselective since it lacks the charged residue commonly found at the TM2 position -1, which is critical for ion selectivity; ii) the experimentally demonstrated low channel conductance of subunit A might be due to the peculiar presence of three Arg in the MA-helix (R-4', R0' and R4'), which are not found in any of the other subunits.

Furthermore, a physicochemical characterisation of the TM-IC domains of all the 5-HT_3R homopentamers and of several heteropentameric receptors provides a static picture of the environment that an ion encounters when passing through the pore at the TM and IC domain levels and suggests that a negative pore potential surface is required for the ions to enter the channel and cross it. Such a negative potential surface in the 5-HT_3AB receptors is granted by the maximum presence of two B subunits (although some exception might be envisaged). This hypothesis is further confirmed by the analysis of the

energetic profile of a selected ion along the pore channel of 5-HT_3 homopentamer A and B and of 5-HT_3AB heteropentamers, estimated by using the Poisson-Boltzmann (PB) equation.

The analyses described were performed by taking into account only the ECD or the TM-IC portions of the receptor separately. However, the local physicochemical properties at the interface between the EC and the TM domains could be sensibly affected by the absence of the missed domain. A complete model of the receptor (i.e. the EC, TM, and IC domains) embedded into the membrane might be useful to clarify few unexpected findings (i.e. the "ABABA" and "AAABB" heteropentamers pore profile) and peculiar cases (i.e. the potential functionality of the "BBABA" heteropentamers, for which the analysis of the electrostatic properties drawn to contrasting conclusions). Moreover, molecular dynamics experiments performed on the whole receptor system would allow to identify possible conformational changes in the receptor, providing new insights into the understanding of its functionality.

Further experimental analyses will be necessary to shed new light on this complex issue, to verify the hypotheses supported here and to validate and improve the computational approach used in the study of the 5-HT_3 receptor. For instance, mutagenesis experiments on the subunits C, D and E performed on the important residues of the ECD (i.e. "hot core" residues) could provide important information about their role in ligand binding. Moreover, other and deeper studies carried out on the different heteromeric receptors using the AFM, might clarify the disagreement arisen about the stoichiometry of the heteromeric 5-HT_3AB receptor, and show the possible stoichiometry of the other heteromeric receptors (5-HT_3AC, 5-HT_3AD and 5-HT_3E).